difference in clinical features.[8,11,12] Two reasons for this similarity in terms of clinical features could be suggested. First, the mosaic ratio might be different in each organ. Because aberrant methylation was generally partial, it would occur after fertilization, and the patients would be mosaic. A high mosaic ratio would be a critical factor in the emergence of a distinct phenotype in BWS patients with monolocus methylation defects. Second, the imprinted locus at 11p15 might be epidominant over other imprinted loci because all MMD patients were clinically diagnosed as BWS.

Regarding the causative factor(s) for MMD, we could not find any pathological variation in any aberrantly methylated DMR, including *Kv*DMR1, suggesting that *cis*-acting variations of each specific DMR itself were not involved in the genesis of MMDs. On the other hand, the involvement of *trans*-acting factors has been advocated in other reports because mutations of *ZFP57* (which are required for the postfertilization maintenance of maternal and paternal methylation imprinting at multiple loci) have been found in transient neonatal diabetes mellitus type 1 patients with multilocus hypomethylation.[32] Mutations of *NLRP2* were also identified in a BWS patient with *Kv*DMR1-LOM and *MEST*-LOM in a family with complex consanguinity and in a Silver–Russell syndrome patient with multilocus hypomethylation.[12,33] In addition, TRIM28, NLRP7, KHDC3L, and DNMT3L have been considered to be candidate *trans*-acting factors. However, no mutations in any of these candidates or other genes, such as *DNMT1*, *DNMT3A*, and *DNMT3B*, were found in our BWS patients with MMDs, as determined by exome sequencing (K. Sasaki and K. Hata, personal communication). Recently, Lorthongpanich et al.[34] reported that the absence of maternal *Trim28* until zygotic gene activation at the two-cell late stage caused mosaicism of MMDs randomly, suggesting that insufficient expression of the candidate gene(s) at very early embryogenesis is an important event in the generation of MMDs in human imprinted diseases. Whole-genome sequencing and whole-genome bisulfite sequencing, including the regulatory regions of the candidate genes, and transcriptome analysis in early embryogenesis would be useful to identify the cause(s) of MMDs.

In our *H19*DMR-GOM patients, we also found GOM of *IGF2*-DMR0 and *IGF2*-DMR2 to be associated with GOM of *H19*DMR and *H19promoter* DMR, in agreement with previous reports.[22,35,36] Two patients showed simultaneous GOM at both *IGF2*-DMRs. Because *Igf2*-DMRs were established at the postimplantation stage under the control of *H19*DMR in mice,[37] GOM of *IGF2*-DMRs in BWS is likely to occur at the same stage. Although the function of *IGF2*-DMR0 is still unknown, methylated *Igf2*-DMR2 plays a role in transcription initiation of *Igf2* in mice.[38] GOM of the DMRs might change the high-order chromatin structure of the maternal allele and increase the expression of *IGF2* in cooperation with *H19*DMR-GOM in BWS patients.

In conclusion, our comprehensive and quantitative methylation analysis of multiple imprinted DMRs revealed several new findings: (i) matDMRs, probably gametic maternally methylated DMRs, are more susceptible to aberrant methylation during the preimplantation stage, when *Kv*DMR1-LOM occurs; (ii) aberrant methylation indeed alters imprinted gene expression; and (iii) *cis*-acting pathological variations of each DMR are not involved in the MMDs analyzed. Moreover, our study confirmed the simultaneous aberrant hypermethylation of *IGF2*-DMR0 and/or -DMR2 with isolated *H19*DMR-GOM. These findings may help us to understand the molecular mechanisms and pathophysiological features of MMDs.

SUPPLEMENTARY MATERIAL

Supplementary material is linked in the online version of the paper at http://www.nature.com/gim.

ACKNOWLEDGMENTS

We thank all the participants and their families who provided samples and all the doctors who referred patients to us. This study was supported, in part, by a Grant for Research on Intractable Diseases from the Ministry of Health, Labor, and Welfare; a Grant for Child Health and Development from the National Center for Child Health and Development; a Grant-in-Aid for Challenging Exploratory Research; and a Grant-in-Aid for Scientific Research (C) from the Japan Society for the Promotion of Science.

DISCLOSURE

The authors declare no conflict of interest.

REFERENCES

1. Abramowitz LK, Bartolomei MS. Genomic imprinting: recognition and marking of imprinted loci. *Curr Opin Genet Dev* 2012;22:72–78.
2. Tomizawa S, Sasaki H. Genomic imprinting and its relevance to congenital disease, infertility, molar pregnancy and induced pluripotent stem cell. *J Hum Genet* 2012;57:84–91.
3. Weksberg R, Shuman C, Beckwith JB. Beckwith-Wiedemann syndrome. *Eur J Hum Genet* 2010;18:8–14.
4. Choufani S, Shuman C, Weksberg R. Beckwith-Wiedemann syndrome. *Am J Med Genet C Semin Med Genet* 2010;154C:343–354.
5. Soejima H, Higashimoto K. Epigenetic and genetic alterations of the imprinting disorder Beckwith-Wiedemann syndrome and related disorders. *J Hum Genet* 2013;58:402–409.
6. Mackay DJ, Boonen SE, Clayton-Smith J, et al. A maternal hypomethylation syndrome presenting as transient neonatal diabetes mellitus. *Hum Genet* 2006;120:262–269.
7. Rossignol S, Steunou V, Chalas C, et al. The epigenetic imprinting defect of patients with Beckwith-Wiedemann syndrome born after assisted reproductive technology is not restricted to the 11p15 region. *J Med Genet* 2006;43:902–907.
8. Bliek J, Verde G, Callaway J, et al. Hypomethylation at multiple maternally methylated imprinted regions including PLAGL1 and GNAS loci in Beckwith-Wiedemann syndrome. *Eur J Hum Genet* 2009;17:611–619.
9. Azzi S, Rossignol S, Steunou V, et al. Multilocus methylation analysis in a large cohort of 11p15-related foetal growth disorders (Russell Silver and Beckwith Wiedemann syndromes) reveals simultaneous loss of methylation at paternal and maternal imprinted loci. *Hum Mol Genet* 2009;18:4724–4733.
10. Lim D, Bowdin SC, Tee L, et al. Clinical and molecular genetic features of Beckwith-Wiedemann syndrome associated with assisted reproductive technologies. *Hum Reprod* 2009;24:741–747.
11. Poole RL, Docherty LE, Al Sayegh A, et al.; International Clinical Imprinting Consortium. Targeted methylation testing of a patient cohort broadens the epigenetic and clinical description of imprinting disorders. *Am J Med Genet A* 2013;161:2174–2182.
12. Court F, Martin-Trujillo A, Romanelli V, et al. Genome-wide allelic methylation analysis reveals disease-specific susceptibility to multiple methylation defects in imprinting syndromes. *Hum Mutat* 2013;34:595–602.

13. Tee L, Lim DH, Dias RP, et al. Epimutation profiling in Beckwith-Wiedemann syndrome: relationship with assisted reproductive technology. *Clin Epigenetics* 2013;5:23.
14. DeBaun MR, Tucker MA. Risk of cancer during the first four years of life in children from The Beckwith-Wiedemann Syndrome Registry. *J Pediatr* 1998;132(3 Pt 1):398–400.
15. Soejima H, Nakagawachi T, Zhao W, et al. Silencing of imprinted CDKN1C gene expression is associated with loss of CpG and histone H3 lysine 9 methylation at DMR-LIT1 in esophageal cancer. *Oncogene* 2004;23:4380–4388.
16. Higashimoto K, Nakabayashi K, Yatsuki H, et al. Aberrant methylation of H19-DMR acquired after implantation was dissimilar in soma versus placenta of patients with Beckwith-Wiedemann syndrome. *Am J Med Genet A* 2012;158A:1670–1675.
17. Yatsuki H, Higashimoto K, Jozaki K, et al. Novel mutations of CDKN1C in Japanese patients with Beckwith-Wiedemann syndrome. *Genes & Genomics* 2013;35:141–147.
18. Higashimoto K, Jozaki K, Kosho T, et al. A novel de novo point mutation of the OCT-binding site in the IGF2/H19-imprinting control region in a Beckwith-Wiedemann syndrome patient. *Clin Genet* 2013; e-pub ahead of print 8 November 2013.
19. Ehrich M, Nelson MR, Stanssens P, et al. Quantitative high-throughput analysis of DNA methylation patterns by base-specific cleavage and mass spectrometry. *Proc Natl Acad Sci USA* 2005;102:15785–15790.
20. Rumbajan JM, Maeda T, Souzaki R, et al. Comprehensive analyses of imprinted differentially methylated regions reveal epigenetic and genetic characteristics in hepatoblastoma. *BMC Cancer* 2013;13:608.
21. Cui H, Onyango P, Brandenburg S, Wu Y, Hsieh CL, Feinberg AP. Loss of imprinting in colorectal cancer linked to hypomethylation of H19 and IGF2. *Cancer Res* 2002;62:6442–6446.
22. Murrell A, Ito Y, Verde G, et al. Distinct methylation changes at the IGF2-H19 locus in congenital growth disorders and cancer. *PLoS One* 2008;3: e1849.
23. Woodfine K, Huddleston JE, Murrell A. Quantitative analysis of DNA methylation at all human imprinted regions reveals preservation of epigenetic stability in adult somatic tissue. *Epigenetics Chromatin* 2011;4:1.
24. Reik W, Maher ER. Imprinting in clusters: lessons from Beckwith-Wiedemann syndrome. *Trends Genet* 1997;13:330–334.
25. Kobayashi H, Yamada K, Morita S, et al. Identification of the mouse paternally expressed imprinted gene Zdbf2 on chromosome 1 and its imprinted human homolog ZDBF2 on chromosome 2. *Genomics* 2009;93:461–472.
26. Nakabayashi K, Trujillo AM, Tayama C, et al. Methylation screening of reciprocal genome-wide UPDs identifies novel human-specific imprinted genes. *Hum Mol Genet* 2011;20:3188–3197.
27. Liu J, Litman D, Rosenberg MJ, Yu S, Biesecker LG, Weinstein LS. A GNAS1 imprinting defect in pseudohypoparathyroidism type IB. *J Clin Invest* 2000;106:1167–1174.
28. Demars J, Shmela ME, Rossignol S, et al. Analysis of the IGF2/H19 imprinting control region uncovers new genetic defects, including mutations of OCT-binding sequences, in patients with 11p15 fetal growth disorders. *Hum Mol Genet* 2010;19:803–814.
29. Weksberg R, Shuman C, Caluseriu O, et al. Discordant KCNQ1OT1 imprinting in sets of monozygotic twins discordant for Beckwith-Wiedemann syndrome. *Hum Mol Genet* 2002;11:1317–1325.
30. Tost J, Dunker J, Gut IG. Analysis and quantification of multiple methylation variable positions in CpG islands by Pyrosequencing. *Biotechniques* 2003;35:152–156.
31. Claus R, Wilop S, Hielscher T, et al. A systematic comparison of quantitative high-resolution DNA methylation analysis and methylation-specific PCR. *Epigenetics* 2012;7:772–780.
32. Mackay DJ, Callaway JL, Marks SM, et al. Hypomethylation of multiple imprinted loci in individuals with transient neonatal diabetes is associated with mutations in ZFP57. *Nat Genet* 2008;40:949–951.
33. Meyer E, Lim D, Pasha S, et al. Germline mutation in NLRP2 (NALP2) in a familial imprinting disorder (Beckwith-Wiedemann Syndrome). *PLoS Genet* 2009;5:e1000423.
34. Lorthongpanich C, Cheow LF, Balu S, et al. Single-cell DNA-methylation analysis reveals epigenetic chimerism in preimplantation embryos. *Science* 2013;341:1110–1112.
35. Reik W, Brown KW, Schneid H, Le Bouc Y, Bickmore W, Maher ER. Imprinting mutations in the Beckwith-Wiedemann syndrome suggested by altered imprinting pattern in the IGF2-H19 domain. *Hum Mol Genet* 1995;4:2379–2385.
36. Sparago A, Russo S, Cerrato F, et al. Mechanisms causing imprinting defects in familial Beckwith-Wiedemann syndrome with Wilms' tumour. *Hum Mol Genet* 2007;16:254–264.
37. Lopes S, Lewis A, Hajkova P, et al. Epigenetic modifications in an imprinting cluster are controlled by a hierarchy of DMRs suggesting long-range chromatin interactions. *Hum Mol Genet* 2003;12:295–305.
38. Murrell A, Heeson S, Bowden L, et al. An intragenic methylated region in the imprinted Igf2 gene augments transcription. *EMBO Rep* 2001;2:1101–1106.

Endocrine
DOI 10.1007/s12020-014-0434-4

RESEARCH LETTER

Hypogonadotropic hypogonadism in a female patient previously diagnosed as having waardenburg syndrome due to a sox10 mutation

Yoko Izumi · Ikuma Musha · Erina Suzuki · Manami Iso · Tomoko Jinno · Reiko Horikawa · Shin Amemiya · Tsutomu Ogata · Maki Fukami · Akira Ohtake

Received: 6 June 2014 / Accepted: 19 September 2014

Introduction

Hypogonadotropic hypogonadism (HH) is a clinically and genetically heterogeneous condition that can be associated with several additional clinical features such as anosmia, cleft palate, and hearing loss [1]. HH with anosmia is referred to as Kallmann syndrome (KS). More than 20 genes are known to underlie HH and/or KS, although mutations in these genes account for only a minor portion of the etiology of HH/KS [1–4]. In 2013, Pingault et al. identified *SOX10* mutations in seven patients with KS [5]. Furthermore, Pingault et al. found that genetic knockout of *Sox10* disrupted migration of GnRH cells in murine fetuses [5]. Subsequently, Vaaralahti et al. identified an additional KS patient with a *SOX10* mutation [6]. These results indicate that *SOX10* mutations constitute rare genetic causes of KS. Currently, *SOX10* is known as one of the causative genes of Waardenburg syndrome (WS), a rare genetic disorder characterized by hearing loss and hypopigmentation in the skin, hair, and eye [7]. Indeed, hearing impairment with or without gray/white hair was found in most of the KS cases reported by Pingault et al. and Vaaralahti et al. [5, 6]. However, detailed clinical assessment of the *SOX10* mutation-positive patients and functional assays of the *SOX10* mutants remain fragmentary. Thus, genetic links between HH/KS and WS have not been fully established. Here, we performed molecular and clinical analyses of a previously reported patient with WS due to a frameshift mutation in *SOX10*.

Patient

The patient was first described in 2008 as an infant with WS-type 2 (WS without dystopia canthorum) [8]. Shortly after birth, she presented with hypopigmented irides and a

Yoko Izumi, Ikuma Musha, and Erina Suzuki contributed equally to this work.

Electronic supplementary material The online version of this article (doi:10.1007/s12020-014-0434-4) contains supplementary material, which is available to authorized users.

Y. Izumi · E. Suzuki · M. Iso · T. Jinno · T. Ogata · M. Fukami (✉)
Department of Molecular Endocrinology, National Research Institute for Child Health and Development, 2-10-1 Ohkura, Setagaya, Tokyo 157-8535, Japan
e-mail: fukami-m@ncchd.go.jp

Y. Izumi
Department of Obstetrics and Gynecology, Keio University School of Medicine, 35 Shinanomachi, Shinjuku, Tokyo 160-8582, Japan

I. Musha · S. Amemiya · A. Ohtake
Department of Pediatrics, Faculty of Medicine, Saitama Medical University, 38 Morohongo Moroyama-machi, Iruma-Gun, Saitama 350-0495, Japan

R. Horikawa
Department of Endocrinology and Metabolism, National Center for Child Health and Development, 2-10-1 Ohkura, Setagaya, Tokyo 157-8535, Japan

T. Ogata
Department of Pediatrics, Hamamatsu University School of Medicine, 1-20-1 Handayama, Higashi-ku, Hamamatsu, Shizuoka 431-3192, Japan

Published online: 02 October 2014

piece of white forelock. Dystopia canthorum, broad nasal root, limb anomaly, and Hirschsprung disease were absent. Ophthalmologic examinations revealed bilateral ocular albinism with hypopigmented fundus and hypochromic iris. Auditory brainstem response indicated bilateral sensorineural deafness. The patient underwent cochlear implantation at 2.6 years of age. Direct sequence analysis of WS causative genes (*SOX10, PAX3*, *MITF* and *SNAI2*) identified a heterozygous mutation in *SOX10* (c.506delC, p.P169fsX117) and excluded mutations in the other genes [8]. Until nine years of age, her growth followed the −1.0 standard deviation (SD) growth curve of Japanese female population. Thereafter, the SD scores for height and height velocity gradually decreased.

At 12.9 years of age, she revisited our clinic because of delayed puberty. Physical examination revealed mild short stature (−2.1 SD) and a lack of pubertal signs (breast and pubic hair, Tanner stage 1) (Figure S1). A smell test using intravenous injection of combined vitamins (Alinamin, Takeda Pharmaceutical Co. Ltd., Japan) [9] induced no response. Other standard smell tests such as UPSIT were not performed. Her bone age was delayed (~11 years of age). Endocrine studies revealed a low level of estradiol (E_2), together with apparently normal gonadotropin levels at the baseline and after GnRH stimulation (Table 1). The blood values of other hormones were grossly normal; whereas the TSH response to TRH was blunted, normal levels of thyroid hormones suggested preserved thyroid function [10, 11]. Low E_2 levels and normal gonadotropin levels were also observed in examinations performed at 13.8 and 14.1 years of age (Table 1). Brain magnetic resonance imaging (MRI) was not performed, because her cochlear implants contained magnetic components. From 14.1 years of age, she received E_2 supplementation therapy, which successfully induced breast budding and improved height growth (Figure S1). To confirm the genetic basis of HH in this patient, we performed further molecular analyses.

Methods

This study was approved by the Institutional Review Board Committee at the National Center for Child Health and Development and performed after obtaining informed consent. Mutation screening was carried out for the coding regions of 20 causative genes for HH/KS: *CHD7*, *FGF8*, *FGFR1*, *FSHB*, *GNRH1*, *GNRHR*, *HS6ST1*, *KAL1*, *KISS1*, *KISS1R*, *LEP*, *LEPR*, *LHB*, *NELF*, *PROK2*, *PROKR2*, *SEMA3A*, *TAC3*, *TACR3*, and *WDR11* [2, 4]. Nucleotide alterations were determined by the Haloplex system (Agilent Technologies, Palo Alto, CA, USA) on a MiSeq sequencer (Illumina, San Diego, CA, USA). Genome-wide copy-number analysis was performed by oligoarray-based comparative genomic hybridization using an array-based catalog CGH (4 × 180 k format, catalog number G4449A; Agilent Technologies).

In vitro reporter assays for the *SOX10* mutation were carried out by a previously reported method with slight modifications [12, 13]. An expression vector for wildtype *SOX10* was purchased from Kazusa DNA Research Institute (Kisarazu, Chiba, Japan). An expression vector for the mutant *SOX10* was generated by site-directed mutagenesis. A luciferase reporter vector containing the *MITF* promoter sequence (–2253 to +97 bp) and an expression vector for *PAX3* [12, 13] were kindly provided by Dr. Bondurand and Professor Goossens. Transient transfection was performed using HEK293 cells seeded in 24-well plates (1.0×10^5 cells/well) and Lipofectamine 2000 Reagent (Life technologies, Carlsbad, CA, USA), with the expression vectors (20 ng/well or 40 ng/well), the luciferase reporter vector (10 ng/well), and a pCMV-PRL internal control vector (5 ng/well; Promega, Madison, WI, USA). As controls for the expression vectors, an empty counterpart vector (HaloTag vector, Promega) was transfected. At 48 h after transfection, the cells were harvested and subjected to luciferase analysis using the dual luciferase reporter assay system and GloMax Luminometer (Promega). Luciferase assays were also performed with co-expression of a *PAX3* expression vector (20 ng/well). These experiments were carried out in triplicate within a single experiment and the experiment was repeated four times. Statistical significance was determined by the *t* test.

To predict the pathogenicity of the *SOX10* mutation, we performed direct sequencing of *SOX10* for the samples obtained from the clinically normal parents of the patient. In this experiment, we used previously described primers [8].

Results

Mutation screening excluded mutations in other HH/KS-associated genes. Comparative genomic hybridization analysis detected no pathogenic copy-number alterations. The mutant SOX10 protein barely transactivated the *MITF* promoter and exerted no dominant-negative effect on wildtype SOX10 (Figure S2). The *SOX10* mutation was not detected in the parental samples.

Discussion

Herein, we report a female patient who developed HH. Although standard smell tests and brain MRI were not performed for the patient, the lack of response to

Table 1 Endocrine data of the patient

Hormone	Stimulus (dosage)	Patient		Reference values[a]	
		Baseline	Peak	Baseline	Peak
At 12.9 years of age					
LH (mIU/ml)	GnRH (100 μg)[b]	1.0	11.8	0.4–4.1	8.5–15.5
FSH (mIU/ml)	GnRH (100 μg)[b]	2.6	13.2	4.8–10.4	8.3–20.0
Estradiol (pg/ml)		<10		<10–144	
GH (ng/ml)	Insulin (3 U)[b]	3.74	**4.83**[c]	0.3–33.1	>6.0
GH (ng/ml)	Arginine (18 g)[d]	4.2	9.7	0.3–33.1	>6.0
Prolactin (ng/ml)	TRH (350 μg)[b]	25.2	43.1	1.2–13.2	2.4–52.8
TSH (μIU/ml)	TRH (350 μg)[b]	1.64	**5.08**	0.32–4.0	10–35
ACTH (pg/ml)	Insulin (3 U)[b]	55.8	88.4	5.2–38.8	10.4–116.4
Cortisol (μg/dl)	Insulin (3 U)[b]	25.2	29.8	3.0–12.0	6.0–36.0
IGF-1 (ng/ml)		205		206–731	
Free T_3 (pg/ml)		3.94		2.43–4.48	
Free T_4 (ng/dl)		1.05		0.98–1.90	
At 13.8 years of age					
LH (mIU/ml)	GnRH (100 μg)[b]	1.0	12.3	0.2–2.1	1.7–5.0
FSH (mIU/ml)	GnRH (100 μg)[b]	2.6	11.6	0.6–3.4	1.4–11.5
Estradiol (pg/ml)		**<10**		12–162	
At 14.1 years of age					
LH (mIU/ml)	GnRH (100 μg)[b]	0.6	10.0	0.2–2.1	1.7–5.0
FSH (mIU/ml)	GnRH (100 μg)[b]	2.5	10.5	0.6–3.4	1.4–11.5
Estradiol (pg/ml)	hMG (150 U)[e]	**<10**	430	13–174	300–1000

The conversion factors to the SI unit: LH, 1.0 (IU/liter); FSH, 1.0 (IU/liter); GH, 1.0 (μg/liter); prolactin, 43.48 (pmol/liter); TSH, 1.0 (mIU/liter); ACTH, 0.22 (pmol/liter); cortisol, 27.59 (nmol/liter), estradiol, 3.671 (pmol/liter); free T_3, 1.536 (pmol/liter); free T_4, 0.1287 (pmol/liter)

Hormone values below the reference range are boldfaced

[a] Reference values in age-matched Japanese females [10, 11]

[b] GnRH, insulin, and TRH i.v.; blood sampling at 0, 30, 60, 90, and 120 min

[c] Low GH may be due to insufficient hypoglycemic stimulation

[d] Arginine i.v.; blood sampling at 0, 30, 60, 90, and 120 min

[e] hMG i.m. for 4 consecutive days; blood sampling on days 1 and 4

intravenous injection of combined vitamins indicated impaired olfactory function. In infancy, the patient was diagnosed as having WS due to a *SOX10* mutation [8]. In the present study, we performed further molecular analysis of the patient and excluded mutations in other HH/KS-associated genes and copy-number alterations in the genome. Furthermore, we confirmed that the *SOX10* mutation is not shared by the clinically normal parents and that the mutant SOX10 has impaired transactivating activity for the *MITF* promoter. These results indicate that the phenotype of this patient results from the *SOX10* mutation. However, we cannot exclude the possibility that the patient has an additional mutation in a hitherto unknown HH/KS-causative gene, because several unidentified genes seem to underlie HH/KS [2–4]. To date, hypogonadism is known as a relatively rare complication in patients with WS due to *SOX10* mutation/deletion [14]. Furthermore, hearing loss was observed in most of the previously reported patients with KS and *SOX10* mutations [5, 6], although hypopigmentation in the eye or skin were not described in these individuals. Our data, together with the previous findings, indicate that *SOX10* mutations can lead to various developmental defects including an overlapping phenotype of HH/KS and WS. Therefore, thorough clinical evaluations including hormonal assessment should be performed for WS patients with *SOX10* mutations, because subnormal gonadotropin secretion may account for a certain fraction of such patients.

It is worth mentioning that our patient showed normal gonadotropin responses to GnRH stimulation and a normal estrogen response to human menopausal gonadotropin stimulation. Thus, hypothalamic dysfunction appears to be the primary lesion of this patient. These results are consistent with the previously proposed notion that SOX10

plays a critical role in the development of hypothalamic neurons [5]. *SOX10* mutations are likely to cause gonadotropin deficiency as a sole hormonal defect, because the levels of blood hormones except for E_2 remained grossly normal in our patient.

The results of in vitro assays suggest that *SOX10* mutations lead to the disease phenotype by haploinsufficiency rather than by dominant-negative effects. The broad phenotypic variation of *SOX10* mutation-positive patients can be explained by the notion that haploinsufficiency of developmental genes is usually associated with a wide range of penetrance and expressivity [15].

In conclusion, the present study provides evidence that *SOX10* haploinsufficiency underlies a continuum of developmental defects that includes both HH and WS. Hypothalamic dysfunction appears to be the major hormonal defect resulting from *SOX10* mutations. Further studies will clarify the prevalence and clinical characteristics of *SOX10* abnormalities.

Acknowledgments We thank Dr. Nadege Bondurand and Professor Michel Goossens for providing us the *MITF* reporter vector and the *PAX3* expression vector.

This study was supported by grants from the Ministry of Health, Labor and Welfare, and from Takeda Science Foundation, by Grants-in-Aid for Scientific Research from the Japan Society for the Promotion of Science and from the Ministry of Education, Culture, Sports, Science, and Technology, and by the Grant of National Center for Child Health and Development.

Conflict of interest All the authors declare that there is no conflict of interest.

References

1. R. Rapaport, Disorders of the gonads, in *Nelson textbook of pediatrics*, 18th edn., ed. by R.M. Kliegman, R.E. Behrman, H.B. Jenson, B.F. Stanton (Saunders, Philadelphia, 2007), pp. 2374–2403
2. L.C. Layman, The genetic basis of female reproductive disorders: etiology and clinical testing. Mol. Cell. Endocrinol. **370**(1–2), 138–148 (2013)
3. H. Miraoui, A.A. Dwyer, G.P. Sykiotis, L. Plummer, W. Chung, B. Feng, A. Beenken, J. Clarke, T.H. Pers, P. Dworzynski, K. Keefe, M. Niedziela, T. Raivio, W.F.Jr Crowley, S.B. Seminara, R. Quinton, V.A. Hughes, P. Kumanov, J. Young, M.A. Yialamas, J.E. Hall, G.V. Vliet, J.P. Chanoine, J. Rubenstein, M. Mohammadi, P.S. Tsai, Y. Sidis, K. Lage, N. Pitteloud, Mutations in FGF17, IL17RD, DUSP6, SPRY4, and FLRT3 are identified in individuals with congenital hypogonadotropic hypogonadism. Am. J. Hum. Genet. **92**(5), 725–743 (2013)
4. Y. Izumi, E. Suzuki, S. Kanzaki, S. Yatsuga, S. Kinjo, M. Igarashi, T. Maruyama, S. Sano, R. Horikawa, N. Sato, K. Nakabayashi, K. Hata, A. Umezawa, T. Ogata, Y. Yoshimura, M. Fukami, Genome-wide copy number analysis and systematic mutation screening in 58 patients with hypogonadotropic hypogonadism. Fertil. Steril. (2014). doi:10.1016/j.fertnstert.2014.06.017
5. V. Pingault, V. Bodereau, V. Baral, S. Marcos, Y. Watanabe, A. Chaoui, C. Fouveaut, C. Leroy, O. Vérier-Mine, C. Francannet, D. Dupin-Deguine, F. Archambeaud, F.J. Kurtz, J. Young, J. Bertherat, S. Marlin, M. Goossens, J.P. Hardelin, C. Dodé, N. Bondurand, Loss-of-function mutations in SOX10 cause Kallmann syndrome with deafness. Am. J. Hum. Genet. **92**(5), 707–724 (2013)
6. K. Vaaralahti, J. Tommiska, V. Tillmann, N. Liivak, J. Känsäkoski, E.M. Laitinen, T. Raivio, De novo SOX10 nonsense mutation in a patient with Kallmann syndrome and hearing loss. Pediatr. Res. (2014). doi:10.1038/pr.2014.60
7. V. Pingault, D. Ente, F. Dastot-Le Moal, M. Goossens, S. Marlin, N. Bondurand, Review and update of mutations causing Waardenburg syndrome. Hum. Mutat. **31**(4), 391–406 (2010)
8. M. Iso, M. Fukami, R. Horikawa, N. Azuma, N. Kawashiro, T. Ogata, SOX10 mutation in Waardenburg syndrome type II. Am. J. Med. Genet. A. **146A**(16), 2162–2163 (2008)
9. M. Furukawa, M. Kamide, T. Miwa, R. Umeda, Significance of intravenous olfaction test using thiamine propyldisulfide (Alinamin) in olfactometry. Auris Nasus Larynx **15**(1), 25–31 (1988)
10. T. Tanaka: Endocrine examination. In: T. Tanaka (ed.) New pocket guide of clinical standard values for children. 1st ed., 106-132. Jihou, Tokyo, (2009) [In Japanese]
11. H. Inada, T. Imamura, R. Nakajima: Assessment of pituitary function. In; H. Inada, T. Imamura, R. Nakajima (eds.) Manual of endocrine examinations of children. 2nd ed., 5-22. Medical Review, Osaka, (2002) [In Japanese]
12. N. Bondurand, V. Pingault, D.E. Goerich, N. Lemort, E. Sock, C.L. Caignec, M. Wegner, M. Goossens, Interaction among SOX10, PAX3 and MITF, three genes altered in Waardenburg syndrome. Hum. Mol. Genet. **9**(13), 1907–1917 (2000)
13. H. Zhang, H. Chen, H. Luo, J. An, L. Sun, L. Mei, C. He, L. Jiang, W. Jiang, K. Xia, J.D. Li, Y. Feng, Functional analysis of Waardenburg syndrome-associated PAX3 and SOX10 mutations: report of a dominant-negative SOX10 mutation in Waardenburg syndrome type II. Hum. Genet. **131**(3), 491–503 (2012)
14. B. Jelena, L. Christina, V. Eric, Q.R. Fabiola, Phenotypic variability in Waardenburg syndrome resulting from a 22q12.3-q13.1 microdeletion involving SOX10. Am. J. Med. Genet A. **164**(6), 1512–1519 (2014)
15. E. Fisher, P. Scambler, Human haploinsufficiency-one for sorrow, two for joy. Nat. Genet. **7**(1), 5–7 (1994)

Journal of Human Genetics (2014), 1–5

www.nature.com/jhg

SHORT COMMUNICATION

Silver–Russell syndrome without body asymmetry in three patients with duplications of maternally derived chromosome 11p15 involving *CDKN1C*

Shinichi Nakashima[1], Fumiko Kato[1], Tomoki Kosho[2], Keisuke Nagasaki[3], Toru Kikuchi[4], Masayo Kagami[5], Maki Fukami[5] and Tsutomu Ogata[1]

We report duplications of maternally derived chromosome 11p15 involving *CDKN1C* encoding a negative regulator for cell proliferation in three Japanese patients (cases 1 and 2 from family A and case 3 from family B) with Silver–Russell syndrome (SRS) phenotype lacking hemihypotrophy. Chromosome analysis showed 46,XX,der(16)t(11;16)(p15.3;q24.3)mat in case 1, 46, XY,der(16)t(11;16)(p15.3;q24.3)mat in case 2 and a *de novo* 46,XX,der(17)t(11;17)(p15.4;q25.3) in case 3. Genomewide oligonucleotide-based array comparative genomic hybridization, microsatellite analysis, pyrosequencing-based methylation analysis and direct sequence analysis revealed the presence of maternally derived extra copies of the distal chromosome 11p involving the wild-type *CDKN1C* (a ~7.98 Mb region in cases 1 and 2 and a ~4.43 Mb region in case 3). The results, in conjunction with the previous findings in patients with similar duplications encompassing *CDKN1C* and in those with intragenic mutations of *CDKN1C*, imply that duplications of *CDKN1C*, as well as relatively mild gain-of-function mutations of *CDKN1C* lead to SRS subtype that usually lack hemihypotrophy.
Journal of Human Genetics (2014) **00**, 1–5. doi:10.1038/jhg.2014.100

INTRODUCTION

Silver–Russell syndrome (SRS) is a congenital developmental disorder characterized by pre- and postnatal growth failure, relative macrocephaly, hemihypotrophy and fifth-finger clinodactyly.[1] Recent studies have shown that epimutation (hypomethylation) of the paternally derived *H19*-differentially methylated region (DMR) at the imprinting control region 1 (ICR1) on chromosome 11p15.5 and maternal uniparental disomy 7 account for ~45 and ~5% of SRS patients, respectively.[1] Thus, underlying (epi)genetic factors still remain to be clarified in a substantial fraction of SRS patients, although several rare (epi)genetic aberrations have been identified in a small fraction of SRS patients.[1]

CDKN1C (cyclin-dependent kinase inhibitor 1C) is a maternally expressed gene that resides at the ICR2 just proximal to the ICR1.[2] *CDKN1C* encodes a negative regulator for cell proliferation and, consistent with this, loss-of-function mutations of *CDKN1C* cause Beckwith–Wiedemann syndrome associated with overgrowth.[2,3] Furthermore, recent studies have shown that gain-of-function mutations of *CDKN1C* result in IMAGe syndrome (IMAGeS) characterized by intrauterine growth restriction, metaphyseal dysplasia, adrenal hypoplasia congenita and male genital abnormalities,[2] whereas less severe gain-of-function mutations of *CDKN1C* have been identified in a large family with maternally inherited SRS.[4] Thus, it has been suggested that relatively severe and mild *CDKN1C* gain-of-function effects lead to IMAGeS and SRS, respectively.[4,5] Notably, IMAGeS patients satisfy the diagnostic criteria for SRS proposed by Nechine *et al.*[5,6] and IMAGeS and SRS patients with *CDKN1C* mutations invariably lack hemihypotrophy characteristic of SRS.[4–6]

Here, we report three patients with SRS and duplications of maternally derived chromosome 11p15.5 involving *CDKN1C*. The results, in conjunction with previous findings, imply that duplications of *CDKN1C*, as well as relatively mild gain-of-function mutations of *CDKN1C* lead to SRS subtype that usually lack hemihypotrophy.

CASE REPORTS

Patients

We studied three Japanese patients (cases 1–3) from two families (Figure 1). Cases 1–3 satisfied the SRS diagnostic criteria proposed by Netchine *et al.*,[6] although they lacked hemihypotrophy (Table 1, see its footnote for Netchine SRS criteria). Oligohydramnios characteristic of SRS[7] was also noticed during the pregnancies of cases 2 and 3. They exhibited no IMAGeS-like phenotypes such as radiologically discernible skeletal dysplasia, an episode suggestive of adrenal dysfunction or undermasculinized genitalia in male case 2.

[1]Department of Pediatrics, Hamamatsu University School of Medicine, Hamamatsu, Japan; [2]Department of Human Genetics, Shinshu University School of Medicine, Matsumoto, Japan; [3]Department of Pediatrics, Niigata University School of Medicine, Niigata, Japan; [4]Department of Pediatrics, Saitama Medical University, Saitama, Japan and [5]Department of Molecular Endocrinology, National Research Institute for Child Health and Development, Tokyo, Japan
Correspondence: Professor T Ogata, Department of Pediatrics, Hamamatsu University School of Medicine, 1-20-1, Handayama, Higashi-ku, Hamamatsu, Shizuoka 431-3192, Japan.
E-mail: tomogata@hama-med.ac.jp
Received 10 October 2014; revised 28 October 2014; accepted 31 October 2014

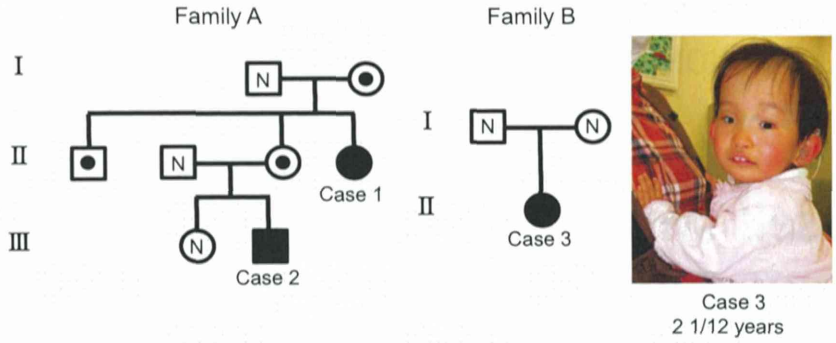

Figure 1 The pedigrees of families A and B and a photograph of case 3. In family A, cases 1 and 2 have an unbalanced translocation involving the distal part of chromosome 11p, the mothers of cases 1 and 2, as well as the brother of case 1 have a balanced translocation involving the distal part of chromosome 11p and the remaining subjects have a normal karyotype. In family B, case 3 has an unbalanced translocation involving the distal part of chromosome 11p and the parents have a normal karyotype. Case 3 exhibits SRS-compatible phenotypes such as prominent forehead, triangular face with relative macrocephaly and micrognathia, ear anomalies and short and curved fifth fingers, but is free from hemihypotrophy.

Table 1 Clinical features of cases 1–3 and reported cases with duplications of maternally derived chromosome 11p15 involving *CDKN1C*

	Case 1 family A female	*Case 2 family A male*	*Case 3 family B female*	*Reported cases (n = 16)*[11–19]
SRS phenotype				
Mandatory criteria for SRS				
BL and/or BW ⩽ −2 SDS	+	+	+	16/16
Scoring system criteria for SRS				
Relative macrocephaly at birth[a]	Unknown	+	+	11/11
PH ⩽ −2 SDS at ⩾2 years	+	Unknown	+	14/14
Prominent forehead	+	+	+	8/9
Body asymmetry	−	−	−	1/15
Feeding difficulties	+	−	Unknown	6/6
Other findings				
Gestational age (weeks)	39	32	32	22–38
Oligohydramnios	Unknown	+	+	Unknown
BL, cm (SDS)	38.0 (−4.9)	34.0 (−3.3)	32.0 (−3.9)	N.D.[b]
BW, kg (SDS)	1.3 (−5.3)	0.87 (−3.6)	0.82 (−3.7)	N.D.[b]
BOFC, cm (SDS)	29.5 (−2.7)	28.3 (−0.6)	27 (−1.2)	N.D.[b]
Present age (years:months)	14:00	1:03	3:03	1–31
PH, cm (SDS)	130.7 (−4.7)	60.8 (−6.4)	70.7 (−6.7)	N.D.[b]
PW, kg (SDS)	37.5 (−1.2)	4.8 (−5.3)	6.8 (−4.0)	N.D.[b]
BMI, kg m^{-2} (SDS)	22.0 (0.7)	13.1 (−2.8)	13.6 (−1.5)	N.D.[b]
POFC, cm (SDS)	Unknown	45.0 (−0.5)	48.5 (−0.1)	N.D.[b]
Relative macrocephaly at present[c]	Unknown	+	+	14/15
Triangular face	−	+	+	12/16
Ear anomalies	−	−	+	8/11
Irregular teeth	Unknown	+	+	1/2
Clinodactyly	+	+	+	10/11
Brachydactyly	+	+	−	4/5
Simian crease	+	+	−	1/2
Muscular hypotonia	Unknown	+	+	4/7
Developmental/speech delay	+	+	+	11/15
IMAGe syndrome phenotype				
IUGR	+	+	+	16/16
Metaphyseal dysplasia	−	−	−	Not described
Adrenal hypoplasia	−	−[d]	−[e]	Not described
Genital abnormality	Female	−	Female	Not described

The diagnosis of Silver–Russell syndrome is made when a patient is positive for the mandatory criteria and at least three of the five scoring system criteria (Netchine *et al*.[5])
Abbreviations: BL, birth length; BMI, body mass index; BOFC, birth occipitofrontal circumference; BW, birth weight; IMAGe, intrauterine growth restriction, metaphyseal dysplasia, adrenal hypoplasia congenita and male genital abnormalities; IUGR, intrauterine growth retardation; N.D., not determined; PH, present height; POFC, present occipitofrontal circumference; PW, present weight; SDS, standard deviation score.
For reported cases, the denominators indicate the number of patients examined for the presence or absence of each feature, and the numerators represent the number of patients assessed to be positive for that feature.
Birth and present body sizes were assessed by the gestational/postnatal age- and sex-matched Japanese reference data from the Ministry of Health, Labor and Welfare and from the Ministry of Education, Science, Sports and Culture.
[a]BL or BW (SDS)—BOFC (SDS) ⩽ −1.5.
[b]N.D. because of various ethnicities of affected individuals and descriptions of height assessment (percentile and SDS).
[c]PH or PW (SDS)—POFC (SDS) ⩽ −1.5.
[d]A rapid adrenocorticotropin stimulation test (0.25 mg m^{-2} bolus i.v.; blood sampling at 0 and 60 min) showed a sufficient cortisol response (14.2 → 26.2 μg dl^{-1}) (reference range >20 μg dl^{-1}).
[e]A growth hormone releasing peptide 2 stimulation test (2 μg kg^{-1} bolus i.v.; blood sampling at 0, 15, 30, 45 and 60 min) yielded a sufficient cortisol response (18.4 → 25.5 μg dl^{-1}).

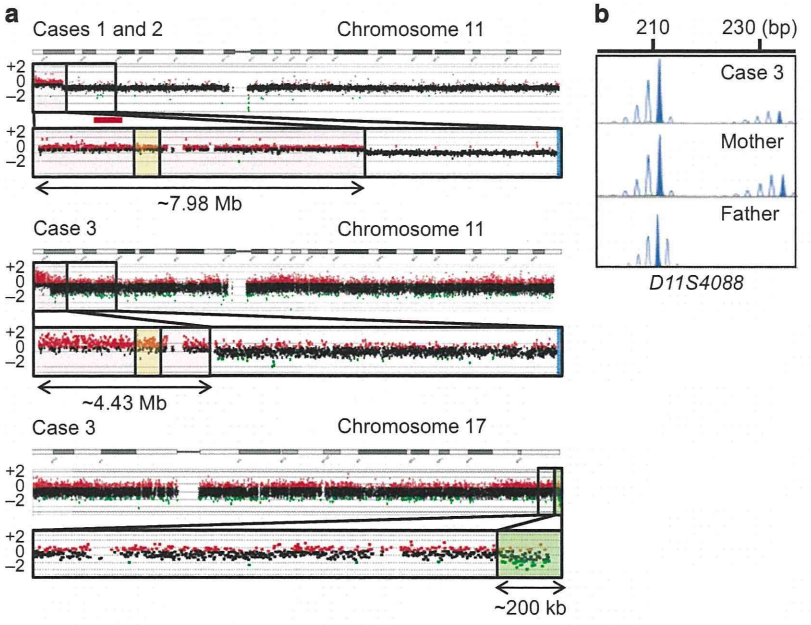

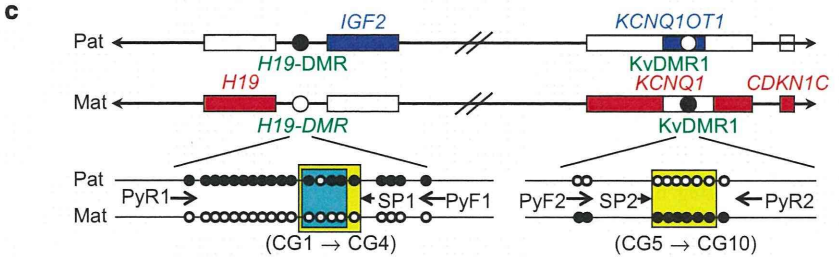

	Case 1			Case 2			Case 3			Controls (n=50)
	P	F	M	P	F	M	P	F	M	Median (Range)
CG1	30	41	53	34	52	55	29	44	44	45 (36 ~ 55)
CG2	31	42	54	37	54	55	28	43	44	46 (36 ~ 57)
CG3	33	45	56	38	57	60	31	47	46	50 (39 ~ 64)
CG4	33	44	55	39	56	57	31	48	46	48 (37 ~ 60)
CG5	72	56	56	72	56	57	68	56	57	58 (49 ~ 66)
CG6	78	59	59	73	59	60	71	61	58	61 (52 ~ 68)
CG7	67	52	50	66	50	52	61	50	49	48 (41 ~ 54)
CG8	69	55	53	68	53	55	63	52	52	48 (42 ~ 55)
CG9	78	60	61	75	63	61	72	63	59	67 (55 ~ 72)
CG10	74	63	57	79	60	59	77	63	64	64 (55 ~ 71)

Figure 2 Representative molecular findings. (**a**) Array comparative genomic hybridization analysis. The black, red and green dots represent signals indicative of the normal, increased (log2 signal ratio > +0.5) and decreased (log2 signal ratio < −0.8) copy numbers, respectively. The log2 signal ratios of +0.5 and −1.0 indicate the presence of three copies and a single copy of the corresponding regions, respectively. The red and the green rectangles represent increased and decreased copy number regions, respectively. The yellow rectangles denote the regions encompassing the ICR1 and the ICR2. (**b**) Microsatellite analysis for *D11S4088* proximal to the KvDMR1. Unequal amplification of the heterozygous peaks in each subject is consistent with short products being more easily amplified than long products and comparison of area under curves of the 212 bp and the 234 bp alleles between case 3 and the mother indicates the presence of two 212 bp alleles and a single 234 bp allele in case 3. This implies that the maternal 212 and 234 bp alleles and the paternal 212 bp allele have been transmitted to case 3. (**c**) Pyrosequencing-based methylation analysis of the *H19*-DMR at the ICR1 and the KvDMR1 at the ICR2, using bisulfite-treated genomic DNA. The cytosine residues at the CpG dinucleotides within the *H19*-DMR is methylated after paternal transmission (filled circles) and unmethylated after maternal transmission (open circles), whereas those within the KvDMR1 is unmethylated after paternal transmission (open circles) and methylated after maternal transmission (filled circles). Paternally and maternally expressed genes are shown in blue and red, respectively. For the *H19*-DMR, a segment encompassing 21 CpG dinucleotides was PCR amplified with PyF1 and PyR1 primers and a sequence primer (SP1) was hybridized to a single-stranded PCR product. Subsequently, the MIs were obtained for four CpG dinucleotides (CG1–CG4) (indicated with a yellow rectangle). The blue rectangle indicates the CTCF binding site 6. The CpG dinucleotide between CG1 and CG2 was not examined, because it constitutes a C/T SNP (indicated with gray circles). The KvDMR1 was similarly examined using PyF2 and PyR2 primers and SP2 and the MIs were obtained for CG5–CG10. The MIs are summarized in the bottom table. F, father; and M, mother; P, patient.

Cytogenetic and molecular studies

This study was approved by the Institute Review Board Committee at Hamamatsu University School of Medicine and was performed using peripheral leukocyte samples and primers shown in Supplementary Table S1 after obtaining written informed consent. The methods for molecular studies were as reported previously.[7] We also obtained written informed consent to publish the facial photograph of case 3 from the parents.

Chromosome analysis showed 46,XX,der(16)t(11;16)(p15.3;q24.3)mat in case 1, 46,XY,der(16)t(11;16)(p15.3;q24.3)mat in case 2 and a *de novo* 46,XX, der(17)t(11;17)(p15.4;q25.3) in case 3 (Figure 1). Then, genomewide oligonucleotide-based array comparative genomic hybridization was carried out using a catalog human array (2×400 K format, ID G4448A) (Agilent Technologies), revealing the presence of three copies of the distal parts of chromosome 11p involving the ICR1 and the ICR2 in cases 1–3 (a ~7.98 Mb region in cases 1 and 2 and a ~4.43 Mb region in case 3) (Figure 2a). No discernible deletion was identified on the distal chromosome 16q in cases 1 and 2, indicating the position of the chromosome 16q breakpoint at the very telomeric portion, whereas a ~200 kb deletion was detected in the telomeric portion of chromosome 17q in case 3. There was no other copy number alteration that was not registered in the Database of Genomic Variants (http://dgv.tcag.ca/dgv/app/home). Microsatellite analysis was carried out for four loci on the duplicated chromosome 11p, showing the presence of two alleles of maternal origin and a single allele of paternal origin in cases 1–3 (Figure 2b and Supplementary Table S2). Subsequently, pyrosequencing-based methylation analysis was performed for four CpG dinucleotides (CG1–CG4) within the *H19*-DMR and six CpG dinucleotides (CG5–CG10) within the KvDMR1 using bisulfite-treated leukocyte genomic DNA samples and methylation index (MI, the ratio of methylated clones) was obtained for each of CG1–CG10 using PyroMark Q24 (Qiagen) (Figure 2c). In cases 1–3, the MIs for CG1–CG4 were mildly decreased or around the lower limit of the normal range and those for CG5–CG10 were mildly increased or around the upper limit of the normal range. Direct sequence analysis showed no discernible mutation on the *CDKN1C* coding region.

DISCUSSION

Cases 1–3 had SRS without hemihypotrophy (body asymmetry) in the presence of maternally derived extra copies of the distal chromosome 11p involving the ICR1 and the ICR2. This implies that the SRS phenotype lacking hemihypotrophy in cases 1–3 is primarily caused by two copies of maternally expressed genes on the two ICRs. In this regard, of duplicated maternally expressed genes, *CDKN1C* functions as a negative growth regulator[8] and *CDKN1C* gain-of-function mutations have been identified in SRS and IMAGeS,[2,4,5] whereas neither *H19* nor *KCNQ1* appears to have a positive role in growth regulation. Indeed, *H19* is regarded as a possible tumor suppressor gene[9] and *KCNQ1* encoding a voltage-gated potassium channel is involved in cardiac arrhythmias.[10] Thus, it is likely that SRS phenotype lacking hemihypotrophy in cases 1–3 is primarily caused by the presence of two functional copies of the wild-type *CDKN1C*. It should be pointed out, however, that although the der(16)t(11;16)(p15.3;q24.3) chromosome in cases 1 and 2 had no discernible chromosome 16q deletion, the der(17)t(11;17)(p15.4;q25.3) chromosome in case 3 was missing the ~200 kb telomeric 17q region that harbors several genes. In addition, there are multiple nonimprinted genes on the duplicated chromosome 11p15 regions. Thus, altered dosage of such genes may have exerted a certain effect on growth patterns of cases 1–3.

An extra copy of maternally derived chromosome 11p15 involving *CDKN1C* has been identified in 16 patients (Table 1) (for detailed clinical features of each case, see Supplementary Table S3).[11–19] Notably, although they frequently show SRS-like phenotype, hemihypotrophy (body asymmetry) has been found only in a single case[12] and none of them exhibit IMAGeS-like skeletal, adrenal or genital manifestation. This provides further support for the notion that two copies of maternally derived *CDKN1C*, as well as mild gain-of-function mutations of *CDKN1C* usually lead to SRS subtype lacking hemihypotrophy.

CONFLICT OF INTEREST

The authors declare no conflict of interest.

ACKNOWLEDGEMENTS

This work was supported by Grants-in-Aid for Scientific Research (A) (25253023) and Research (B) (23390083) from the Japan Society for the Promotion of Science, by Grants for Research on Intractable Diseases (H22-161) from the Ministry of Health, Labor and Welfare (MHLW) and by Grant for National Center for Child Health and Development (25-10).

1 Eggermann, T. Russell-Silver syndrome. *Am. J. Med. Genet. C Semin. Med. Genet.* **154C**, 355–364 (2010).
2 Arboleda, V.A., Lee, H., Parnaik, R., Fleming, A., Banerjee, A. & Ferraz-de-Souza, B. *et al.* Mutations in the PCNA-binding domain of CDKN1C cause IMAGe syndrome. *Nat. Genet.* **44**, 788–792 (2012).
3 Soejima, H. & Higashimoto, K. Epigenetic and genetic alterations of the imprinting disorder Beckwith–Wiedemann syndrome and related disorders. *J. Hum. Genet.* **58**, 402–409 (2013).
4 Brioude, F., Oliver-Petit, I., Blaise, A., Praz, F., Rossignol, S. & Le Jule, M. *et al.* CDKN1C mutation affecting the PCNA-binding domain as a cause of familial Russell Silver syndrome. *J. Med. Genet.* **50**, 823–830 (2013).
5 Kato, F., Hamajima, T., Hasegawa, T., Amano, N., Horikawa, R. & Nishimura, G. *et al.* IMAGe syndrome: clinical and genetic implications based on investigations in three Japanese patients. *Clin. Endocrinol.* **80**, 706–713 (2014).
6 Netchine, I., Rossignol, S., Dufourg, M. N., Azzi, S., Rousseau, A. & Perin, L. *et al.* 11p15 imprinting center region 1 loss of methylation is a common and specific cause of typical Russell-Silver syndrome: clinical scoring system and epigenetic-phenotypic correlations. *J. Clin. Endocrinol. Metab.* **92**, 3148–3154 (2007).
7 Fuke, T., Mizuno, S., Nagai, T., Hasegawa, T., Horikawa, R. & Miyoshi, Y. *et al.* Molecular and clinical studies in 138 Japanese patients with Silver–Russell syndrome. *PLoS ONE* **8**, e60105 (2013).
8 Lee, M. H., Reynisdottir, I. & Massague, J. Cloning of p57(KIP2), a cyclin-dependent kinase inhibitor with unique domain structure and tissue distribution. *Genes Dev.* **9**, 639–649 (1995).
9 Hao, Y., Crenshaw, T., Moulton, T., Newcomb, E. & Tycko, B. Tumour-suppressor activity of H19 RNA. *Nature* **365**, 764–767 (1993).
10 Wang, Q., Curran, M. E., Splawski, I., Burn, T. C., Millholland, J. M. & VanRaay, T. J. *et al.* Positional cloning of a novel potassium channel gene: KVLQT1 mutations cause cardiac arrhythmias. *Nat. Genet.* **12**, 17–23 (1996).
11 Fisher, A. M., Thomas, N. S., Cockwell, A., Stecko, O., Kerr, B. & Temple, I. K. *et al.* Duplications of chromosome 11p15 of maternal origin result in a phenotype that includes growth retardation. *Hum. Genet.* **111**, 290–296 (2002).
12 Eggermann, T., Meyer, E., Obermann, C., Heil, I., Schüler, H. & Ranke, M. B. *et al.* Is maternal duplication of 11p15 associated with Silver–Russell syndrome? *J. Med. Genet.* **42**, e26 (2005).
13 Schönherr, N., Meyer, E., Roos, A., Schmidt, A., Wollmann, H. A. & Eggermann, T. *et al.* The centromeric 11p15 imprinting centre is also involved in Silver–Russell syndrome. *J. Med. Genet.* **44**, 59–63 (2007).
14 South, S. T., Whitby, H., Maxwell, T., Aston, E., Brothman, A. R. & Carey, J. C. Co-occurrence of 4p16.3 deletions with both paternal and maternal duplications of 11p15: modification of the Wolf–Hirschhorn syndrome phenotype by genetic alterations predicted to result in either a Beckwith–Wiedemann or Russell–Silver phenotype. *Am. J. Med. Genet. A* **146A**, 2691–2697 (2008).
15 Bliek, J., Snijder, S., Maas, S. M., Polstra, A., van der Lip, K. & Alders, M. *et al.* Phenotypic discordance upon paternal or maternal transmission of duplications of the 11p15 imprinted regions. *Eur. J. Med. Genet.* **52**, 404–408 (2009).

16 Eggermann, T., Spengler, S., Bachmann, N., Baudis, M., Mau-Holzmann, U. A. & Singer, S. *et al.* Chromosome 11p15 duplication in Silver-Russell syndrome due to a maternally inherited translocation t(11;15). *Am. J. Med. Genet. A* **152A**, 1484–1487 (2010).
17 Cardarelli, L., Sparago, A., De Crescenzo, A., Nalesso, E., Zavan, B. & Cubellis, M. V. *et al.* Silver-Russell syndrome and Beckwith–Wiedemann syndrome phenotypes associated with 11p duplication in a single family. *Pediatr. Dev. Pathol.* **13**, 326–330 (2010).
18 Bonaldi, A., Mazzeu, J. F., Costa, S. S., Honjo, R. S., Bertola, D. R. & Albano, L. M. *et al.* Microduplication of the ICR2 domain at chromosome 11p15 and familial Silver-Russell syndrome. *Am. J. Med. Genet. A* **155A**, 2479–2483 (2011).
19 Chiesa, N., De Crescenzo, A., Mishra, K., Perone, L., Carella, M. & Palumbo, O. *et al.* The KCNQ1OT1 imprinting control region and non-coding RNA: new properties derived from the study of Beckwith-Wiedemann syndrome and Silver–Russell syndrome cases. *Hum. Mol. Genet.* **21**, 10–25 (2012).

Supplementary Information accompanies the paper on Journal of Human Genetics website (http://www.nature.com/jhg)

Journal of Human Genetics (2014) 59, 353–356

www.nature.com/jhg

SHORT COMMUNICATION

Mutation spectrum and phenotypic variation in nine patients with *SOX2* abnormalities

Junichi Suzuki[1,2], Noriyuki Azuma[3], Sumito Dateki[1,4], Shun Soneda[1], Koji Muroya[5], Yukiyo Yamamoto[6], Reiko Saito[6], Shinichiro Sano[1], Toshiro Nagai[7], Hiroshi Wada[8], Akira Endo[9], Tatsuhiko Urakami[2], Tsutomu Ogata[1,10] and Maki Fukami[1]

Multiple mutations in *SOX2* have been identified in patients with ocular anomalies and/or pituitary dysfunction. Here, we identified *SOX2* abnormalities in nine patients. The molecular defects included one missense, one nonsense and four frameshift mutations, and three submicroscopic deletions involving *SOX2*. Three of the six mutations and all deletions were hitherto unreported. The breakpoints determined in one deletion were located within *Alu* repeats and accompanied by an overlap of 11 bp. Three of the six mutations encoded SOX2 proteins that lacked *in vitro* transactivation activity for the *HESX1* promoter, whereas the remaining three generated proteins with ~15–~20% of transactivation activity. All cases manifested ocular anomalies of various severities, together with several complications including arachnoid cyst and hamartoma. There was no apparent correlation between the residual activity and clinical severity. The results indicate that molecular defects in *SOX2* are highly variable and include *Alu* repeat-mediated genomic rearrangements. Our data provide further evidence for wide phenotypic variation of *SOX2* abnormalities and the lack of genotype–phenotype correlation in patients carrying *SOX2* lesions.
Journal of Human Genetics (2014) **59**, 353–356; doi:10.1038/jhg.2014.34; published online 8 May 2014

Keywords: anophthalmia; deletion; genotype-phenotype correlation; microphthalmia; mutation; SOX2

SOX2 (NP_003097.1) has a critical role in the development of the eye, pituitary and central nervous system through transactivation of multiple genes including *HESX1*.[1–3] Haploinsufficiency of *SOX2* (NM_003106.3) leads to anophthalmia/microphthalmia and pituitary dysfunction, in addition to various neuronal defects such as mental retardation, brain malformation and hearing loss.[3–7] Although >80 patients with *SOX2* abnormalities have been reported to date,[3–11] current understanding of mutation spectrum and phenotypic determinants of this condition remains fragmentary. In fact, *in vitro* functional assays have been performed only for a small number of mutations.[3,11–13] Furthermore, whereas Kelberman *et al.*[12] found no obvious genotype–phenotype correlation, Schneider *et al.*[14] reported that patients with missense mutations had milder ocular phenotypes than those with nonsense or frameshift mutations.

Here, we identified *SOX2* abnormalities in nine patients (cases 1–9). This study was approved by the Institutional Review Board Committee at the National Center for Child Health and Development and performed after obtaining written informed consent. Molecular defects in cases 1–9 were identified through sequencing and copy number analyses of *SOX2* for 37 patients with ocular anomalies and 15 patients with pituitary dysfunction and normal eyes (Supplementary Table S1). Mutations in the coding region were examined by direct sequencing, and copy number abnormalities were analyzed by multiplex ligation-dependent amplification and array comparative genomic hybridization. Detailed methods are provided in Supplementary Table S2. Cases 1–6 carried heterozygous intragenic mutations, whereas cases 7–9 had heterozygous submicroscopic deletions involving *SOX2*. Cases 1–9 invariably manifested developmental defects of eyes, in addition to multiple complications including arachnoid cyst and hamartoma (Table 1 and Supplementary Table S3). The ocular phenotypes included unilateral and bilateral microphthalmia, bilateral coloboma and bilateral anophthalmia. The *SOX2* mutations in cases 1–6 consisted of three previously reported mutations (c.70_89del20, c.70_86del17 and c.480C>G) and three novel mutations (c.235T>C, c.244_245delTT and c.402delC) (Figure 1a). None of the six mutations have been registered as polymorphisms in the single-nucleotide polymorphism database (dbSNP, http://www.ncbi.nlm.nih.gov/). *In vitro* reporter assays using a vector containing the *HESX1* promoter indicated that c.235T>C, c.402delC and c.480C>G encoded proteins with ~15–

[1]National Research Institute for Child Health and Development, Department of Molecular Endocrinology, Tokyo, Japan; [2]Department of Pediatrics and Child Health, Nihon University School of Medicine, Tokyo, Japan; [3]National Center for Child Health and Development, Department of Ophthalmology and Laboratory of Cell Biology, Tokyo, Japan; [4]Department of Pediatrics, Nagasaki University Graduate School of Biomedical Sciences, Nagasaki, Japan; [5]Kanagawa Children's Medical Center, Department of Endocrinology and Metabolism, Yokohama, Japan; [6]Department of Pediatrics, School of Medicine, University of Occupational and Environmental Health, Fukuoka, Japan; [7]Department of Pediatrics, Koshigaya Hospital, Dokkyo Medical University, Koshigaya, Japan; [8]Department of Pediatrics, Yodogawa Christian Hospital, Osaka, Japan; [9]Department of Pediatrics, Iwata City Hospital, Iwata, Japan and [10]Department of Pediatrics, Hamamatsu University School of Medicine, Hamamatsu, Japan
Correspondence: Dr M Fukami, National Research Institute for Child Health and Development, Department of Molecular Endocrinology, Tokyo 157-8535, Japan.
E-mail: fukami-m@ncchd.go.jp
Received 23 January 2014; revised 9 April 2014; accepted 10 April 2014; published online 8 May 2014

Table 1 Molecular and clinical findings of cases 1–9

	Case 1	Case 2	Case 3	Case 4	Case 5	Case 6	Case 7	Case 8	Case 9
Age at examination	3 Months	13 Days	1 Year	19 Years	7 Years	1 Year	12 Years	1 Year	19 Years
Sex	Male	Male	Female	Female	Female	Female	Female	Male	Male
Molecular findings									
SOX2 mutation (cDNA)	c.235T>C	c.480C>G	c.70_89del20[a]	c.70_86del17[b]	c.244_245delTT	c.402delC	Gene deletion	Gene deletion	Gene deletion
SOX2 mutation (protein)	p.W79R	p.Y160X	p.N24fsX88	p.N24fsX89	p.L82fsX94	p.G135fsX153	Deletion	Deletion	Deletion
Parental origin of the mutation/deletion	NE	NE	*De novo*	NE	*De novo*	Father mosaic	NE	NE	*De novo*
In vitro transactivating activity	Hypomorphic	Hypomorphic	Amorphic	Amorphic	Amorphic	Hypomorphic	Null	Null	Null
Clinical findings									
Ocular abnormality (right)	MO	AO	AO	AO	severe MO	MO	severe MO	AO	Retinal fold
Ocular abnormality (left)	Normal	AO	AO	AO	severe MO	MO	severe MO	AO	Optic disc coloboma
Developmental delay	No	Unknown	No	No	Yes	Yes	Yes	Yes	Yes
Prenatal growth	Normal	Normal	Normal	Normal	Normal	Normal	Normal	Normal	LGA
Postnatal growth failure	Yes	Unknown	Yes	Yes	Yes	Yes	Yes	Yes	Normal
Other complication	Esophageal atresia	None	None	None	Hemi-hypertrophy	None	Seizure	None	None
Pituitary hormone deficiency	LH, FSH	NE	NE	LH, FSH, GH	NE	NE	LH, FSH,GH	LH, FSH, GH	LH, FSH
Brain MRI findings	Arachnoid cyst	Dandy–Walker syndrome	Hamartoma	Pituitary hypoplasia	Normal	White matter signal abnormality	Ectopic posterior lobe	Pituitary hypoplasia	NE

Abbreviations: AO, anophthalmia; FSH, follicle-stimulating hormone; GH, growth hormone; LGA, large for gestational age; LH, luteinizing hormone; MO, microphthalmia, MRI, magnetic resonance imaging; NE, not examined.
[a]delAACTCCACCGCGCGCGCGGC.
[b]delAACTCCACCGCGCGCGGC.

~20% transactivation activity, whereas the remaining three generated proteins that lacked the activity (Figure 1b). Of the six mutations, c.70_89del20, c.70_86del17 and c.244_245delTT affected the possible nuclear localization signals predicted from mouse data, and therefore seemed to disturb the intracellular localization of the SOX2 protein (Figure 1a).[15] Furthermore, it remained possible that mRNAs of the nonsense and frameshift mutations undergo early degradation *in vivo*. The deletions in cases 7–9 affected ~1.0 to ~2.5 Mb genomic regions at 3q26-27 including *SOX2*. These deletions overlapped with, but were not identical to, previously reported deletions (Figure 2).[4,7–9,12–14,16] Sequences at the fusion junction were characterized in case 7, showing that the two breakpoints resided within *Alu* repeats and shared an overlap of 11 bp (Figure 2).

Several matters are noteworthy. First, molecular lesions in cases 1–9 were heterogeneous and included six point mutations and three submicroscopic deletions. These data support a broad mutation spectrum of *SOX2* abnormalities.[8,9] Notably, we identified submicroscopic deletions involving *SOX2* in three cases. As multiple microdeletions at 3q26-27 have been reported in patients with ocular anomalies (Figure 2),[4,7–9,12–14,16] it is possible that the genomic region around *SOX2* represents a hotspot for chromosomal rearrangements. In this regard, it is noteworthy that the sequence at the fusion junction in case 7 is consistent with non-allelic homologous recombination that occurs between two homologous sequences or replication-based errors that are usually associated with microhomology at the fusion junction.[17] Furthermore, the two breakpoints of this deletion resided within *Alu* repeats, which facilitate both recombination- and replication-mediated errors.[18,19] These data imply that *Alu* repeats may have a role in the high frequency of deletions at 3q26-27. Second, cases 1–9 manifested several complications in addition to ocular abnormalities. Importantly, seven cases manifested brain anomalies including arachnoid cyst and hamartoma. In this regard, Alatzoglou *et al.*[13] recently described pituitary tumors in two patients with *SOX2* haploinsufficiency. Thus, *SOX2* abnormalities seem to be associated with various types of developmental defects and tumors in the brain. Third, *SOX2* lesions were identified in 9 of 37 patients with ocular abnormalities, but were absent from 15 patients with pituitary dysfunction and normal eyes. The results are consistent with the previous reports that *SOX2* abnormalities account for 10–20% of the etiology of anophthalmia/microphthalmia and rarely result in pituitary dysfunction without eye abnormalities.[4,5,8,9,11] These data can be explained by assuming that, during development, the eye is highly sensitive to reduced activity of SOX2. Nevertheless, as gonadotropin deficiency was observed in all of our mutation-positive cases, SOX2 appears to be indispensable for the function of the hypothalamus–pituitary axis. Lastly, no apparent genotype–phenotype correlation was found in our patient cohort. Although ocular phenotypes were relatively mild in cases 1 and 6 with hypomorphic mutations and obviously severe in cases 3 and 4 with amorphic mutations, bilateral anophthalmia was also observed in case 2 with a hypomorphic mutation and mild coloboma with normal visual activity was seen in case 9 with *SOX2* deletion. Similarly, the occurrence of pituitary dysfunction, mental retardation and short stature was not associated with the mutation types. The lack of correlation between residual activity and phenotypic severity is consistent with the previously proposed notion that haploinsufficiency of developmental genes is usually associated with a wide range of penetrance and expressivity.[20]

Collectively, the present study argues for a broad spectrum of *SOX2* lesions and indicates for the first time that *Alu* repeat-mediated genomic rearrangements at 3q26-27 account for a part of the etiology

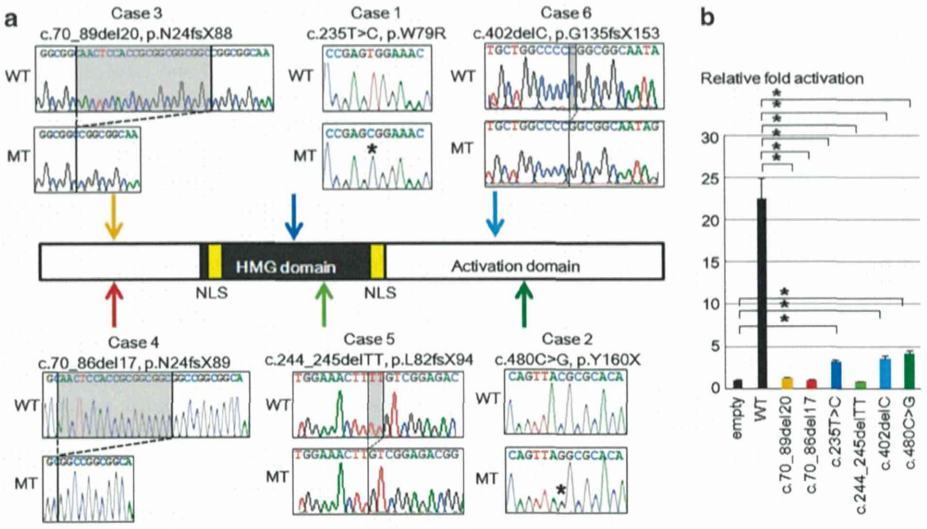

Figure 1 The position and *in vitro* function of *SOX2* mutations identified in the present study. (**a**) Chromatograms of the mutations. Subcloned wild-type (WT) and mutant (MT) sequences are shown. Deleted nucleotides are shaded in gray and mutated nucleotides are indicated by asterisks. The yellow boxes indicate the position of two putative nuclear localization signals (NLSs) predicted from mouse data.[15] (**b**) *In vitro* reporter assay using a luciferase vector containing the *HESX1* promoter. The results are expressed as the mean ± 1 s.d. Asterisks indicate the statistical significance of the results ($P \leqslant 0.05$). The relative fold activation of c.70_89del20, c.70_86del17 and c.244_245delTT was similar to that of the empty vector (empty). The relative percentages of fold activation of c.235T>C, c.402delC and c.480C>G to that of the WT *SOX2* were 13.8%, 15.4% and, 18.4%, respectively.

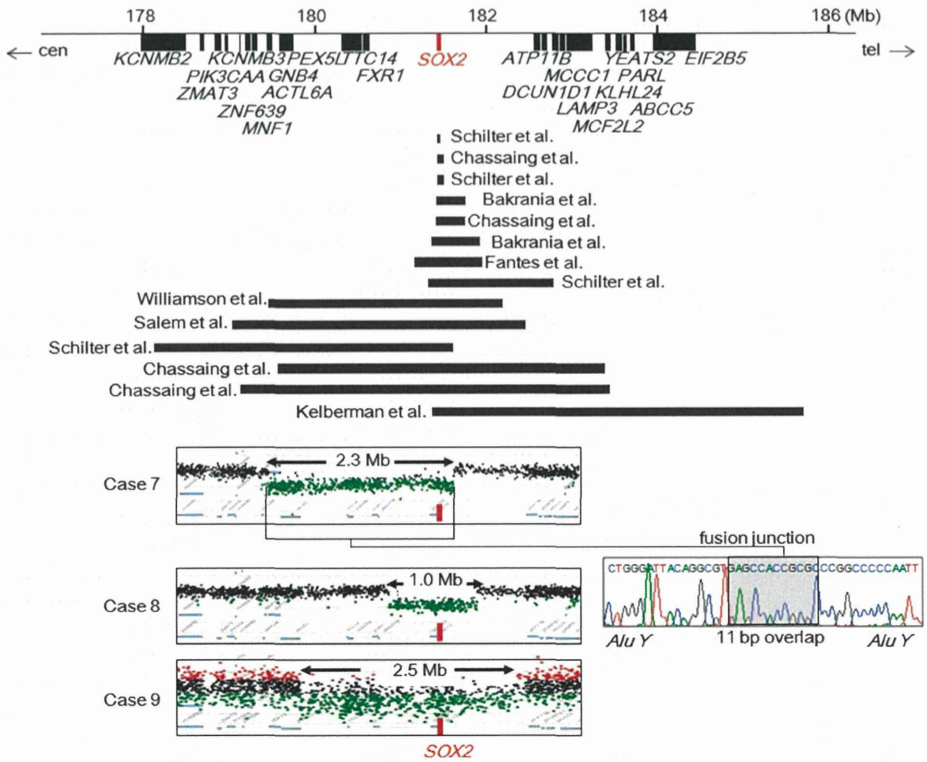

Figure 2 Submicroscopic deletions identified in the present and previous studies. Upper panel: genomic structure of the 3q26-27 region and the position of previously reported deletions. The position of *SOX2* is indicated by a red box and the deletions are depicted by black bars. Genomic positions of the genes and deletions refer to NCBI database (http://www.ncbi.nlm.nih.gov/). Cen, centromere; tel, telomere. Lower panel: comparative genomic hybridization analysis of cases 7–9 from the present study and the sequence at the fusion junction in case 7. The black, red and green dots denote signals indicative of the normal, increased ($> +0.5$) and decreased (< -1.0) copy numbers, respectively. Estimated sizes and positions of the heterozygous deletions are shown.

of *SOX2* haploinsufficiency. Our data provide further evidence for the wide phenotypic variation and the lack of genotype–phenotype correlation in patients with *SOX2* abnormalities.

CONFLICT OF INTEREST

The authors declare no conflict of interest.

ACKNOWLEDGEMENTS

This work was supported by grants from the Ministry of Health, Labor and Welfare and from Takeda Science Foundation, by Grant-in-Aid for Scientific Research from the Japan Society for the Promotion of Science, by Grant-in-Aid for Scientific Research on Innovative Areas from the Ministry of Education, Culture, Sports, Science and Technology and by the Grant of National Center for Child Health and Development.

1 Kelberman, D., Rizzoti, K., Lovell-Badge, R., Robinson, I. C. & Dattani, M. T. Genetic regulation of pituitary gland development in human and mouse. *Endocr. Rev.* **30,** 790–829 (2009).
2 Jayakody, S. A., Andoniadou, C. L., Gaston-Massuet, C., Signore, M., Cariboni, A., Bouloux, P. M. *et al.* SOX2 regulates the hypothalamic-pituitary axis at multiple levels. *J. Clin. Invest.* **122,** 3635–3646 (2012).
3 Kelberman, D., Rizzoti, K., Avilion, A., Bitner-Glindzicz, M., Cianfarani, S., Collins, J. *et al.* Mutations within Sox2/SOX2 are associated with abnormalities in the hypothalamo-pituitary-gonadal axis in mice and humans. *J. Clin. Invest.* **116,** 2442–2455 (2006).
4 Fantes, J., Ragge, N. K., Lynch, S. A., McGill, N. I., Collin, J. R., Howard-Peebles, P. N. *et al.* Mutations in SOX2 cause anophthalmia. *Nat. Genet.* **33,** 461–463 (2003).
5 Stark, Z., Storen, R., Bennetts, B., Savarirayan, R. & Jamieson, R. V. Isolated hypogonadotropic hypogonadism with SOX2 mutation and anophthalmia/microphthalmia in offspring. *Eur. J. Hum. Genet.* **19,** 753–756 (2011).
6 Hagstrom, S. A., Pauer, G. J., Reid, J., Simpson, E., Crowe, S., Maumenee, I. H. *et al.* SOX2 mutation causes anophthalmia, hearing loss, and brain anomalies. *Am. J. Med. Genet. A* **138A,** 95–98 (2005).
7 Williamson, K. A., Hever, A. M., Rainger, J., Rogers, R. C., Magee, A., Fiedler, Z. *et al.* Mutations in SOX2 cause anophthalmia-esophageal-genital (AEG) syndrome. *Hum. Mol. Genet.* **15,** 1413–1422 (2006).
8 Bakrania, P., Robinson, D. O., Bunyan, D. J., Salt, A., Martin, A., Crolla, J. A. *et al.* SOX2 anophthalmia syndrome: 12 new cases demonstrating broader phenotype and high frequency of large gene deletions. *Br. J. Ophthalmol.* **91,** 1471–1476 (2007).
9 Chassaing, N., Causse, A., Vigouroux, A., Delahaye, A., Alessandri, J. L., Boespflug-Tanguy, O. *et al.* Molecular findings and clinical data in a cohort of 150 patients with anophthalmia/microphthalmia. *Clin. Genet.* (e-pub ahead of print 10 September 2013; doi:10.1111/cge.12275).
10 Schilter, K. F., Reis, L. M., Schneider, A., Bardakjian, T. M., Abdul-Rahman, O., Kozel, B. A. *et al.* Whole-genome copy number variation analysis in anophthalmia and microphthalmia. *Clin. Genet.* **84,** 473–481 (2013).
11 Sato, N., Kamachi, Y., Kondoh, H., Shima, Y., Morohashi, K., Horikawa, R. *et al.* Hypogonadotropic hypogonadism in an adult female with a heterozygous hypomorphic mutation of SOX2. *Eur. J. Endocrinol.* **156,** 167–171 (2007).
12 Kelberman, D., de Castro, S. C., Huang, S., Crolla, J. A., Palmer, R., Gregory, J. W. *et al.* SOX2 plays a critical role in the pituitary, forebrain, and eye during human embryonic development. *J. Clin. Endocrinol. Metab.* **93,** 1865–1873 (2008).
13 Alatzoglou, K. S., Andoniadou, C. L., Kelberman, D., Buchanan, C. R., Crolla, J., Arriazu, M. C. *et al.* SOX2 haploinsufficiency is associated with slow progressing hypothalamo-pituitary tumours. *Hum. Mutat.* **32,** 1376–1380 (2011).
14 Schneider, A., Bardakjian, T., Reis, L. M., Tyler, R. C. & Semina, E. V. Novel SOX2 mutations and genotype-phenotype correlation in anophthalmia and microphthalmia. *Am. J. Med. Genet. A* **149A,** 2706–2715 (2009).
15 Li, J., Pan, G., Cui, K., Liu, Y., Xu, S. & Pei, D. A dominant-negative form of mouse SOX2 induces trophectoderm differentiation and progressive polyploidy in mouse embryonic stem cells. *J. Biol. Chem.* **282,** 19481–19492 (2007).
16 Salem, N. J., Hempel, M., Heiliger, K. J., Hosie, S., Meitinger, T. & Oexle, K. Anal atresia, coloboma, microphthalmia, and nasal skin tag in a female patient with 3.5 Mb deletion of 3q26 encompassing SOX2. *Am. J. Med. Genet. A* **161A,** 1421–1424 (2013).
17 Gu, W., Zhang, F. & Lupski, J. R. Mechanisms for human genomic rearrangements. *Pathogenetics* **1,** 4 (2008).
18 Chen, J. M., Cooper, D. N., Férec, C., Kehrer-Sawatzki, H. & Patrinos, G. P. Genomic rearrangements in inherited disease and cancer. *Semin. Cancer Biol.* **20,** 222–233 (2010).
19 Boone, P. M., Liu, P., Zhang, F., Carvalho, C. M., Towne, C. F., Batish, S. D. *et al.* Alu-specific microhomology-mediated deletion of the final exon of SPAST in three unrelated subjects with hereditary spastic paraplegia. *Genet. Med.* **13,** 582–592 (2011).
20 Fisher, E. & Scambler, P. Human haploinsufficiency—one for sorrow, two for joy. *Nat. Genet.* **7,** 5–7 (1994).

Supplementary Information accompanies the paper on Journal of Human Genetics website (http://www.nature.com/jhg)

Novel Insights from Clinical Practice

HORMONE RESEARCH IN PÆDIATRICS

Horm Res Paediatr 2014;81:133–138
DOI: 10.1159/000355279

Received: April 24, 2013
Accepted: August 21, 2013
Published online: January 18, 2014

A Novel Mutation in SOX2 Causes Hypogonadotropic Hypogonadism with Mild Ocular Malformation

Masaki Takagi [a, b] Satoshi Narumi [a] Yumi Asakura [c] Koji Muroya [c]
Yukihiro Hasegawa [b] Masanori Adachi [c] Tomonobu Hasegawa [a]

[a]Department of Pediatrics, Keio University School of Medicine Tokyo, and [b]Department of Endocrinology and Metabolism, Tokyo Metropolitan Children's Medical Center, Tokyo, and [c]Department of Endocrinology and Metabolism, Kanagawa Children's Medical Center, Yokohama, Japan

Established Facts

- Heterozygous *SOX2* mutations have been reported to cause isolated hypogonadotropic hypogonadism (HH) in addition to ocular and brain abnormalities.
- The most common ocular phenotype associated with *SOX2* mutations is a severe bilateral eye defect such as anophthalmia or severe microphthalmia.

Novel Insights

- We report a novel missense *SOX2* (Y110C) mutation in an HH patient with mild ocular malformation, unilateral retinal detachment.
- The findings in this patient emphasize the importance of testing for *SOX2* mutations in HH individuals with mild ocular defects, such as retinal detachment, in the absence of anophthalmia or severe microphthalmia.
- We used a next-generation sequencing strategy to analyze 122 genes associated with congenital endocrine disorders. This approach is new in HH; it has never been reported to our knowledge.

Key Words
SOX2 · Hypogonadotropic hypogonadism · HMG domain · Targeted next-generation sequencing

Abstract
Background: Heterozygous *SOX2* mutations have been reported to cause isolated hypogonadotropic hypogonadism (HH) in addition to ocular and brain abnormalities. ***Objective:*** We report a novel missense *SOX2* (Y110C) mutation in an HH patient with mild ocular malformation. ***Patients:*** The 20-year-old male was referred because of typical signs of complete hypogonadism, with small intrascrotal testes (2 ml), no pubic hair (P1), and a micropenis. Hormone assays revealed very low plasma testosterone levels and very low levels of plasma gonadotropin. He was found to have retinal detachment in his right eye and surgery was performed at the age of 14 years. ***Results:*** Using a next-generation se-

KARGER

E-Mail karger@karger.com
www.karger.com/hrp

1663–2818/14/0812–0133$39.50/0

Tomonobu Hasegawa, MD, PhD
Department of Pediatrics
Keio University School of Medicine, 35 Shinanomachi
Shinjuku-ku, Tokyo 160-8582 (Japan)
E-Mail thaseg@a6.keio.jp

quencing strategy, we identified a novel heterozygous *SOX2* mutation, c.329A>G (p.Y110C). Y110C SOX2 had reduced transactivation and no dominant negative effect. Subcellular localization revealed no significant difference between wild-type and mutant SOX2. EMSA experiments showed that the Y110C SOX2 abrogated DNA-binding ability. ***Conclusion:*** The Y110C mutation affects a critical residue in the SOX2 protein. This study extends our understanding of the phenotypic features, molecular mechanism, and developmental course associated with mutations in *SOX2*. When multiple genes need to be analyzed for mutations simultaneously, targeted sequence analysis of interesting genomic regions is an attractive approach.

Introduction

Hypogonadotropic hypogonadism (HH) is a genetically heterogeneous condition, defined by absent or incomplete sexual maturation secondary to gonadotropin deficiency. Several genes have been linked to the pathogenesis of HH, including *KAL1*, *FGFR1*, *FGF8*, *PROK2*, *PROKR2*, *CHD7*, *GNRHR*, *GNRH1*, *KISS1R*, *KISS1*, *TAC3*, *TACR3*, and *SOX2* [1–8].

Heterozygous mutations in *SOX2* were first reported in patients with bilateral anophthalmia or severe microphthalmia who had additional abnormalities, including developmental delays, learning difficulties, esophageal atresia, and genital abnormalities [9–11]. Subsequently, *SOX2* mutations were also shown to be associated with anterior pituitary hypoplasia, HH, and variable growth hormone deficiency in association with other manifestations, including hippocampal abnormalities, defects of the corpus callosum, hypothalamic hamartoma, and sensorineural hearing loss [7, 8]. To date, more than 40 mutations in *SOX2* have been described [12]. The majority of these are truncating mutations such as nonsense or frameshift mutations, and only 10 missense mutations have been reported.

Here, we report an HH patient with mild ocular phenotypes carrying a novel missense mutation in *SOX2* (Y110C). Through molecular analyses, we showed that substitution of a conserved, critical amino acid near the DNA-binding high-mobility group (HMG) domain of SOX2 abrogated DNA-binding and pituitary gene *(HESX1)* activation. This study extends our understanding of the phenotypic features, molecular mechanism, and developmental course associated with mutations in the *SOX2* gene.

Table 1. Endocrinological findings (baseline) in the propositus

	20 years	Reference (adult)
IGF-1, ng/ml	307	male: 41–369
TSH, μU/ml	2.42	0.3–3.50
Free T4, ng/dl	1.15	1.09–2.55
Free T3, pg/ml	3.82	3.23–5.11
LH, mIU/ml	0.1	male: 2.2–8.4
FSH, mIU/ml	0.31	male: 1.8–12
Testosterone, ng/ml	0.38	male: 2.01–7.50

The conversion factors to the SI units are as follows: IGF-I 0.131 (nmol/l), TSH 1.0 (mIU/l), free T4 12.87 (pmol/l), free T3 1.54 (pmol/l), LH 1.0 (IU/l), FSH 1.0 (IU/l), and testosterone 0.035 (nmol/l).

Materials and Methods

Case Report

The propositus was a 23-year-old Japanese man born at 41 weeks of gestation after an uncomplicated pregnancy and delivery. The parents were nonconsanguineous and phenotypically normal. He had one younger sister who had no relevant clinical problems. His birth weight was 3,250 g (+0.6 SD), and length was 49.0 cm (0.0 SD). He had horizontal nystagmus and bilateral cryptorchidism, which were diagnosed in the first months of life. No anophthalmia or microphthalmia was recorded. His gross motor development was almost normal. At the age of 3 years, he presented with generalized seizures, which have been well controlled with sodium valproate. At the age of 14 years, he was found to have retinal detachment in his right eye and surgery was performed.

He was referred at the age of 20 years due to the typical signs of complete hypogonadism, with small intrascrotal testes (2 ml), no pubic hair (P1), and a micropenis. Hormone assays revealed very low plasma levels of testosterone and gonadotropin (table 1). Brain MRI showed a normal pituitary and olfactory bulb and no other abnormalities. He had a normal sense of smell. His karyotype was 46,XY. His height and weight were 174.4 cm (+0.7 SD) and 63.9 kg (+0.2 SD), respectively. The visual acuity of both his right and left eyes was 0.01 without glasses and 0.6 with glasses.

Mutation Screening

After obtaining informed consent, and with the approval of the Institutional Review Board of Keio University School of Medicine, genomic DNA was extracted from peripheral blood leucocytes of the propositus and his parents. We sequenced 13 genes implicated in HH, including *CHD7*, *FGFR1*, *FGF8*, *GNRH1*, *GNRHR*, *KAL1*, *KISS1*, *KISS1R*, *PROK2*, *PROKR2*, *TAC3*, *TACR3*, and *SOX2* using the MiSeq instrument (Illumina Inc., San Diego, Calif., USA) according to the SureSelect protocol (Agilent Technologies, Santa Clara, Calif., USA). In brief, 3 μg of genomic DNA were used for the SureSelect capture methods. Exons of 122 genes known to be associated with congenital endocrine disorders (including 13 HH-related genes) were identified in the University of California Santa

Cruz table browser (http://genome.ucsc.edu/). In total, we targeted 1,321 regions comprising 246,158 bp using SureSelect. DNA obtained from the SureSelect solution-based sequence capture was subjected to MiSeq sequencing according to the manufacturer's protocol. Base calling, read filtering, and demultiplexing were performed with the standard Illumina processing pipeline. We used BWA 0.6.1 and SAMtools 0.1.18 for alignment and variant detection against the human reference genome (NCBI build 37; hg19) with the default settings. Local realignment, quality score recalibration and variant calling were performed by GATK 2.3.9 with the default settings. We used ANNOVAR for annotation of called variants.

Crystal Structure Modeling

The crystal structure of the SOX2 HMG domain (protein data bank ID 1GT0; http://www.rcsb.org/pdb/) was used as a reference wild-type (WT) structure for modeling the structure of Y110C SOX2 using the PyMOL Molecular Graphics System (http://www.pymol.org).

Functional Studies

To generate SOX2 expression vectors, *SOX2* cDNA was cloned into pCMV-myc (Clontech, Palo Alto, Calif., USA). For subcellular localization analyses, we purchased a Halo-tagged clone vector (Kazusa DNA Research Institute, Chiba, Japan) containing human SOX2 cDNA. We introduced the Y110C mutation by site-directed mutagenesis using the PrimeSTAR Mutagenesis Basal Kit (TaKaRa, Otsu, Japan). A luciferase reporter vector was constructed by inserting the *HESX1* promoter sequence (–405 to +267 bp) into a pGL4.24 [luc2P/minP] vector (Promega, Madison, Wisc., USA). A transactivation assay was performed in HeLa cells using a dual-luciferase reporter assay system (Promega). For subcellular localization analyses, we visualized HeLa cells transfected with Halo-tagged SOX2 and TMRDirect™ ligands (Promega), according to the manufacturer's instructions. We photographed the cells using a Leica TCS-SP5 laser scanning confocal microscope (Leica, Exton, Pa., USA). The sequences of the biotin-labeled double-stranded oligonucleotide used as probe in the EMSA experiment was 5′-CAAACAAATAAACAATTAACTC -3′ [13]. Five micrograms of nuclear protein extraction was incubated at room temperature in a 20-μl binding reaction mixture containing a 20-fmol probe, 50 mM KCl, 5 mM $MgCl_2$, 2.5% glycerol, 0.05% NP-40, and 1 μg poly(dI-dC) for 20 min. For competition experiments, a large excess (200×) of unlabeled competitor oligonucleotides was included in the binding reactions. The protein-DNA complexes were subject to gel electrophoresis and transferred to a nylon membrane. The biotin-labeled probe was detected with the Lightshift Chemiluminescent EMSA Kit (Pierce).

Results

Mutation Screening

We identified a novel heterozygous *SOX2* mutation, c.329A>G (p.Y110C), the only gene among 13 HH-related genes where unknown variants were identified. We used Sanger sequencing of PCR products from genomic DNA to confirm the *SOX2* variant (fig. 1a). Y110 is immediately N-terminal to the DNA-binding HMG domain, which is highly conserved among SOX proteins and is critical for binding to both interacting proteins and target DNA sequences. Y110 is a highly evolutionarily conserved amino acid (fig. 1b), and this mutation was not detected in 150 healthy Japanese controls. No sequence variation was found in *CHD7*, *FGFR1*, *FGF8*, *GNRH1*, *GNRHR*, *KAL1*, *KISS1*, *KISS1R*, *PROK2*, *PROKR2*, *TAC3*, and *TACR3*. Parental analysis was refused.

Crystal Structural Modeling

Y110C SOX2 was predicted to lose a residue-DNA contact (fig. 1c).

Functional Studies

In Hella cells, WT SOX2 stimulated transcription of the *HESX1* reporter in a dose-dependent manner. Y110C SOX2 had reduced transactivation, and had no dominant negative effect (fig. 2a). Subcellular localization revealed no significant difference between WT and mutant SOX2 (fig. 2b), indicating that nuclear targeting was not affected by the mutation. WT SOX2 specifically bound to the DNA and this binding was competed by an excess (200×) of cold competitors. In contrast, Y110C SOX2 had abrogated DNA-binding ability (fig. 2c).

Discussion

We characterized a novel mutant (Y110C) of the SOX2 transcription factor that is associated with HH and a mild ocular phenotype. The Y110C SOX2 protein had abrogated DNA-binding affinity and decreased transcription activity compared to WT SOX2 with no dominant negative effect. The partial transcription activity suggests that the Y110C mutation is a hypomorphic mutation that retains residual activity. The most common ocular phenotype associated with *SOX2* mutations is a severe bilateral eye defect such as anophthalmia or severe microphthalmia. If an eye is present, it may be associated with ocular features, including sclerocornea. Our patient showed only unilateral retinal detachment. This mild phenotype was likely due to residual SOX2 activity. The findings in this patient emphasize the importance of testing for *SOX2* mutations in HH individuals with mild ocular defects, such as retinal detachment, in the absence of anophthalmia or severe microphthalmia.

To date, more than 40 mutations in *SOX2* have been described. Most of the mutations cause premature termination codons as a result of nonsense or frameshift muta-

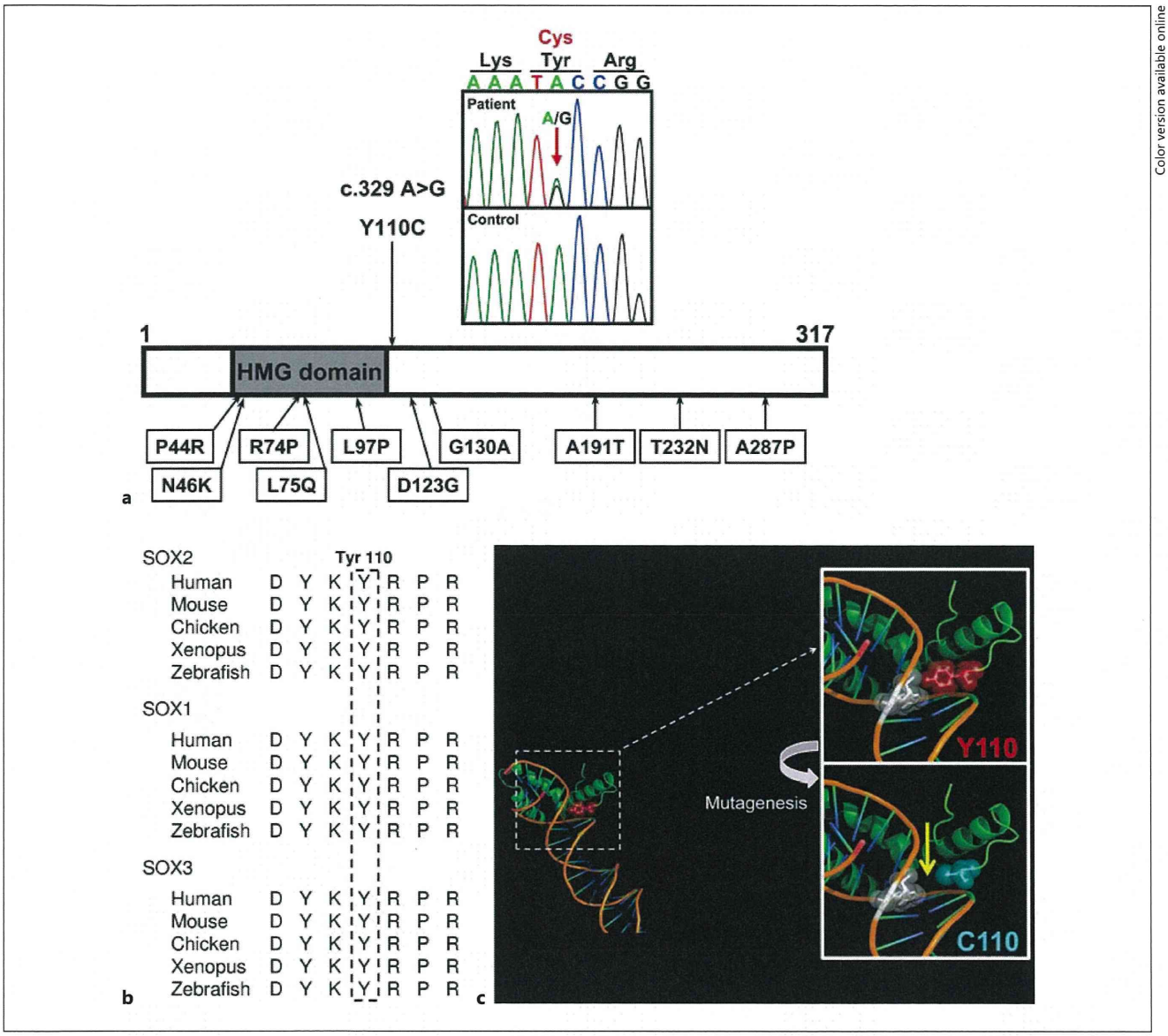

Fig. 1. Identification of sequence variation of *SOX2*. **a** Partial sequence of PCR product and schematic diagrams of the SOX2 protein. The chromatogram represents a heterozygous substitution of cysteine (TGC) in place of tyrosine (TAC) at codon 110. The arrow indicates the mutated nucleotide. Tyrosine 110 is located immediately 3′ of the HMG domain. The reported 10 missense mutations are summarized. **b** Homology study showed tyrosine at codon 110 is highly conserved through species in SOX2, SOX1, and SOX3. **c** Modeled structure of the Y110C in comparison with the WT structure (upper panels). Modeling of the mutant was performed using a built-in mutagenesis function of the PyMOL Molecular Graphics System. Crystal structural modeling showed Y110C SOX2 was predicted to lose a residue-DNA contact (yellow arrow).

tions; only 10 missense mutations have been reported. Among these 10 missense mutations, only 3 (R74P, L75Q, and L97P) have been confirmed as pathogenetic by functional assays [7, 10, 14]. All 3 mutations are located in the HMG domain and cause anophthalmia or severe microphthalmia. Therefore, Y110C is the only amino acid change located outside of the HMG domain that has been shown to be pathogenetic in functional assays.

Recently, Mihelec et al. [15] reported a 4-generation family with marked ocular phenotypic variability harbor-

Horm Res Paediatr 2014;81:133–138
DOI: 10.1159/000355279

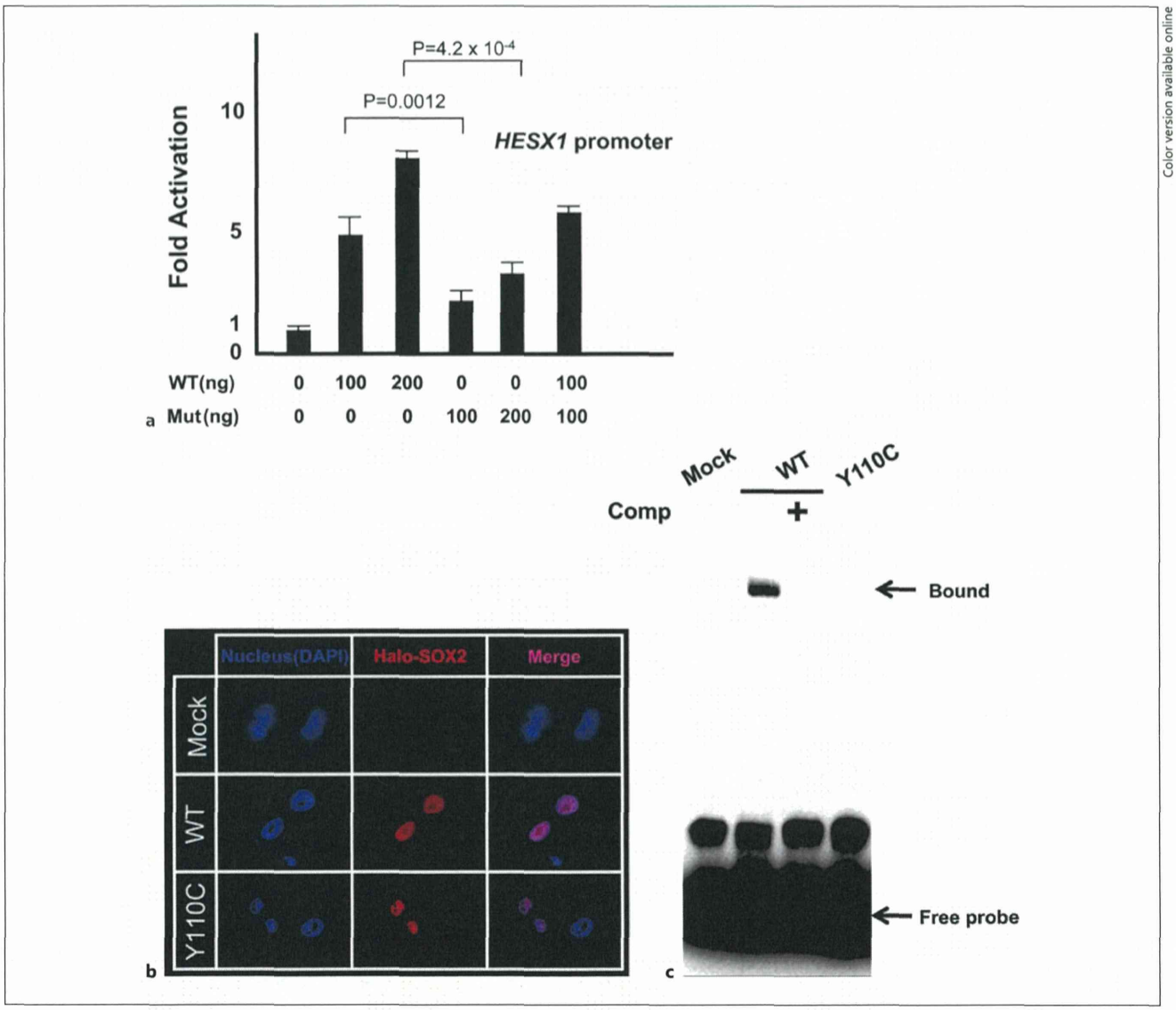

Color version available online

Fig. 2. Functional characterization of Y110C SOX2. **a** Transactivation assays of Y110C SOX2 using *HESX1* reporter Hela cells were cotransfected with the pRL-CMV internal control vector, indicated amount (nanograms) of the effector plasmids, and the *HESX1* reporter. WT SOX2 stimulated transcription of the *HESX1* reporter in a dose-dependent manner. Y110C SOX2 exhibited reduced transactivation and had no dominant negative effect. The data are given as means ± SEM of at least 3 independent experiments performed in triplicate transfections. **b** Subcellular localization analysis. For subcellular localization analyses, we visualized and photographed Hela cells transfected with Halo-tagged SOX2 using a Leica TCS-SP5 laser scanning confocal microscope, after mounting the cells in a Vectashield-DAPI solution. The WT and Y110C SOX2 are localized to the nucleus. **c** EMSA experiments. WT SOX2 showed specific binding to the elements, which was competed by an excess amount of (200×) cold competitors. The Y110C SOX2 showed abrogated DNA-binding ability.

ing a D123G SOX2 mutation. These multigenerational patients suggested that there had been no fertility problems in the carriers of the D123G SOX2 mutation. D123G is located immediately C-terminal to the HMG domain, which was described as a partner-factor interaction region by Mihelec et al. [15]. SOX transcription factors exert tissue-specific effects in concert with tissue-specific partner factors. In the lens, SOX2 interacts with the lens-specific factor δEF3, and this interaction is dependent on the partner-factor interaction region [16]. Y110 is also

Horm Res Paediatr 2014;81:133–138
DOI: 10.1159/000355279